MALEIC ACID AS A VERSATILE CATALYST FOR BIOREFINING

by

Jonathan C. Overton

A Dissertation

Submitted to the Faculty of Purdue University

In Partial Fulfillment of the Requirements for the degree of

Doctor of Philosophy

School of Agricultural and Biological Engineering

West Lafayette, Indiana

May 2020

THE PURDUE UNIVERSITY GRADUATE SCHOOL
STATEMENT OF COMMITTEE APPROVAL

Dr. Nathan S. Mosier, Chair

School of Agricultural and Biological Engineering

Dr. Abigail Engelberth

School of Agricultural and Biological Engineering
Department of Environmental and Ecological Engineering

Dr. Eduardo Ximenes

School of Agricultural and Biological Engineering

Dr. Jeffrey Miller

Davidson School of Chemical Engineering

Approved by:

Dr. Nathan S. Mosier

To my wife, Sabrina, whose love, encouragement, and smile have been the greatest motivation I will ever know.

To my parents, who held me to high standards and always gave me support. They remind me to always strive to achieve my fullest potential.

ACKNOWLEDGMENTS

First and foremost, I would like to thank my advisor Dr. Mosier for his constant advice, support and encouragement throughout the course of my Ph.D. work. He has demonstrated to me how a researcher, leader, and mentor should act.

I would also like to thank my committee members: Drs. Abby Engelberth, Eduardo Ximenes, and Jeff Miller for their feedback, discussions, and input on this work. Drs. Michael Ladisch, Kevin Solomon, Kendra Erk, and Gozdem Kilaz also have contributed notably to my development as a researcher and scholar in my time here. Additionally, the wonderful support staff of ABE have made being a member of the department a true pleasure. The completion of my degree would not have been possible without Carla Carrie, Lindsey Crawley, Linda (Xingya) Liu, Becky Peer, and all the other staff that make ABE great day in and day out. I would like to especially thank Nikki Zimmerman, the graduate program administrator for all her dedication and hard work towards making grad life better for all ABE students. The group of graduate students in the Laboratory of Renewable Resource Engineering (LORRE) at Purdue are among the best out there. I am so thankful to have shared my successes and failures with them as researchers and friends. I will miss coffee breaks and discussions with each of you. In particular, I want to thank Casey Hooker, Jenny Rackliffe, Jessica Yates, Logan Readnour, Pablo Vega, Elena Robles, Ethan Hillman, Kok Zhi, Antonio dos Santos, Emma Brace, Samira Fatemi, Raymond 'Studie' Redcorn, Grace Baldwin, Momo, Lawrence Seku, Didi Ramirez, Julia Burchell, Clark Eby, and Ana Moreno-Martinez for assistance in the lab or just for being solid friends.

During my dissertation work I was fortunate enough to work as an intern at Archer Daniels Midland. I would like to extend a huge thank you to Iman Tabar, Mike Taussig, Rhea Sammons, and Chelsea Schmid for hiring me and investing time and effort into developing my process development skills.

I would also like to thank my family and friends for being such an amazing group of people. Life sure is fun when you're surrounded by such an awesome group of people to give you laughs, advice, and encouragement.

I am sure that I missed somebody, somewhere on this list, so I want to extend a general thank you to all the people I've been surrounded by in my time at Purdue and before. I have had

such an amazing experience and I will cherish my time here. Thank you all for helping to make my journey so enjoyable, educational, and filled with personal growth.

TABLE OF CONTENTS

LIST OF TABLES

LIST OF FIGURES

LIST OF ABBREVIATIONS

ACN	Acetonitrile
$AlCl_3$	Aluminum chloride
CCR	Combined corn refinery
DEE	Diethyl ether, ether
DFF	Diformylfuran
DMF	2,5-dimethylfuran
DMSO	Dimethylsulfoxide
FDCA	Furandicarboxcylic acid
FDME	2,5-furan dicarboxylic acid dimethyl ester
FPU	Filter paper units
HMF	5-hydroxymethylfurfural
HPLC	High performance liquid chromatography
IRR	Internal rate of return
k1	Isomerization rate of glucose to fructose
k2	Dehydration rate of fructose to hmf
k3	Rehydration rate of hmf to lva
k5	Rate of humin formation during isomerization
k6	Rate of humin formation during dehydration
kdis	Rate of glucose consumption
krev	Isomerization rate of fructose to glucose
LVA	Levulinic acid
MD	Molecular dynamics
meTHF	Methyl-tetrahydrofuran
NPV	Net present value
PEF	Poly(ethylene 2,5-furandicarboxylate)
PERT	Program evaluation and review technique
PET	Poly(ethylene terephthalate)
PX	Para xylene
RDF	Radial distribution function
RID	Refractive index detector
ROI	Return on investment
RPM	Rotations per minute
TEA	Techno-economic analysis
TPA	Terephthalic acid

ABSTRACT

Producing bio-based commodity chemicals, such as polymers and fuels, is of significant interest as petroleum reserves continue to decline. A major roadblock to bio-based production is high processing costs. These costs are associated with the need for highly-specialized catalysts to produce bio-based commodity chemicals from agricultural products and wastes. This prevents bioprocessing facilities from fully taking advantage of commodities of scale, where purchasing materials in greater quantities reduces the material cost. Discovering catalysts capable of being used in multiple production pathways could reduce the per unit processing of a biorefinery. Recent works have shown that maleic acid can be used for multiple conversion reactions of plant material to valuable products: xylose to furfural, glucose to hydroxymethylfurfural (HMF), and the pretreatment of lignocellulosic material for second generation biofuel production. This work evaluates the use of maleic acid as a catalyst for producing HMF from corn starch, with a specific focus on reducing operating costs. Additionally, the use of maleic acid as a liquefaction catalyst for producing corn stover slurries is tested.

To evaluate HMF production from starch, a combined computational and experimental approach is used. Through modelling and experimental validation, molar HMF yields of ~30% are reached by incorporating dilute dimethylsulfoxide and acetonitrile into the reaction mixture. However, HMF yield was limited by low stability in the reaction media. The addition of activated carbon to the reactor overcomes challenges with second order side reactions, resulting in HMF selling prices that are competitive with similar petroleum-derived chemicals. The key technical roadblocks to commercialization of HMF production are identified as solvent recycling and HMF separation efficiency in a sensitivity analysis. During liquefaction of corn stover, maleic acid was found to reduce the yield stress required to begin slurry flow through a pipe. However, a reduction in the free water content of the reactor through binding of water in the matrix of biomass limited liquefaction, resulting in solids concentrations not financially feasible at scale. To overcome this, maleic acid treatment was performed at solids contents of 25%, followed by a water removal step and enzymatic liquefaction at 30% solids. Yield stress was reduced from >6000 Pa for untreated samples to ~50 Pa for samples treated with maleic acid and enzymes sequentially. Such treatment reduces the challenges associated with feeding solid biomass into a pretreatment reactor.

Additionally, reduced slurry yield stress results in lower capital costs, since smaller pumps can be used in the production facility.

This work provides a step forward in transitioning away from a petroleum-based economy to a bio-based economy without significant disruptions in product pricing and availability.

1. INTRODUCTION

1.1 Thesis Perspective and Overview

The aim of this dissertation is to evaluate the potential role of maleic acid as a versatile catalyst in the context of a biorefinery. We evaluate two different core uses of maleic acid with respect to processing major agricultural products in the Midwest region of the United States:

1. Production of 5-hydroxymethylfurfural (HMF) from corn-derived starch
2. Creating 'pumpable' slurries of corn stover for second generation biofuel production

The novelty of this research is that we reach very high yields (>80%) of HMF from starch using an aqueous cosolvent solution with the addition of activated carbon. A preliminary economic evaluation of the developed process predicts that HMF produced from this process can be sold for less than \$0.60 lb^{-1}, which is competitive with comparable products produced from petroleum.

Liquefaction of lignocellulosic material for handling in a biorefinery is a relatively new topic. Maleic acid is evaluated for conversion of corn stover into an aqueous liquid slurry. Additionally, the use of enzymes instead of maleic acid is evaluated. The sequential combination of maleic acid liquefaction and enzymatic liquefaction reduces the yield stress of a 30% (w/v) corn stover slurry to 50 Pa. Without treatment, the slurry yield stress is greater than 6000 Pa.

1.2 Biorefineries: Opportunities and Challenges

For the past 100 years, the vast majority of carbon-based product have been derived from petroleum due to low cost and high availability. However, dwindling petroleum reserves and increasing prices have emphasized the need for sustainable and renewable sources of carbon-based products. Biologically-derived carbohydrates stored in the cell walls of plants are among the most abundant carbon sources on earth and make a very promising resource for replacing petroleum-derived products in the global economy. However, widespread utilization of biological carbon has not been achieved for a number of reasons:

1. Many easily accessed carbons, such as starches, are stored in staple food crops such as corn, potatoes, and rice. Growing global population and diminishing increases in

agricultural production result in growing concern regarding competition between food and industry for use of edible biomass.

2. A downside of many biorefinery process is low overall product yield. Chemical methods for refining biomass into products are less selective due to heterogeneity of biomass and often have low (<50%) product yields. Naturally, dedicating material, capital, and operational costs to a material that consists of less than 70% useable sugars by weight drives up the cost of many biorefinery products, reducing competition with petroleum products.
3. A large portion of plant-based carbon that does not compete with food supplies is stored in energy crops and agricultural residues, such as corn stover, also known as lignocellulosic material. While readily available, use of lignocellulosic biomass is greatly inhibited by the recalcitrance of lignin, which acts as a protective sheath to stored sugar polymers. The requirement of pretreatment at elevated (>160 °C) temperatures to disrupt lignin, an upper solid handling limit of ~15% (w/v) for pretreatment, combined with the high (>\$15 kg^{-1}) cost of enzymes provide major bottlenecks to financially competitive operation of a lignocellulosic biorefinery.
4. Currently, design equations for the reactors and pumps in a lignocellulosic biorefinery are not readily available. This provides a limitation to the accuracy of cost modeling and optimization efforts as well as greatly increasing the risk of investment in a biorefinery using lignocellulosic material.

1.3 Research Objectives

The objective of this research is to overcome critical economic barriers preventing the development and operation of bio-derived, commodity production facilities. A literature review will show that costs, mostly associated with catalysts (enzyme or chemical) are major roadblocks to producing economically feasible bioproducts. One strategy to overcome these financial barriers uses economies of scale, where purchasing larger quantities of a material results in a lower price per unit of material. This is, in part, caused by the increased certainty of selling a certain quantity for the supplier. In petroleum-based refineries, purchasing more catalysts means an increase in the rate substrate can be processed. However, as described later in this work, biorefineries are also limited by substrate availability due to the low density of agricultural materials for transport. This

limits the practical area which can be harvested and delivered to a single biorefinery. This has prevented existing biorefinery designs from taking full advantage of economies of scale. In this dissertation, this limitation is overcome through the use of a single chemical catalyst (maleic acid) for multiple processing steps. By using maleic acid to process both corn kernels and corn stover into value-added products, a clear path forward is described to creating an economically-feasible biorefinery in the major corn producing regions of the United States. This dissertation describes experimental data, computational modelling, and analyses that support the following three fundamental hypotheses:

I. Dimethylsulfoxide and acetonitrile as cosolvents increase HMF yield and selectivity through $AlCl_3$ and maleic acid-catalyzed conversion of glucose.

II. Adding activated carbon to HMF reaction media greatly increases molar HMF yield from starch, driving predicted HMF selling price to be competitive with similar petroleum products at ~\$0.55 lb^{-1}.

III. Treating pelletized corn stover with maleic acid at 150 °C for 30 minutes reduced the yield stress of corn stover slurries, resulting in reduced capital requirements for a lignocellulose to ethanol refinery (2^{nd} generation biofuel production).

Hypotheses I and II represent significant improvements in the future outlook of HMF production from starch and glucose. Previously, low reaction yields and substrate loadings had resulted in high operational costs due to challenges with separating dilute HMF and complications from the significant portions of impurities in the reaction product. These high production costs resulted in HMF selling price not being competitive with paraxylene and terephthalic acid, petroleum-derived commodity chemicals that HMF could replace in the economy.

Hypothesis III furthers the understanding of how biomass slurries behave during transport between unit operations in a biorefinery. Additionally, strategies developed from hypothesis III can pave the way for increased facility uptime in biorefineries, a key bottleneck in second generation biofuel production. Proposed future work focuses on overcoming key technical limitations of reactor design and scale-up for these systems, as well as merging practical findings in slurry dynamics with computational fluid dynamics software to better understand the interplay between mass transfer and enzyme kinetics in a stirred tank reactor at high solids loadings.

2. LITERATURE REVIEW

2.1 Introduction

To understand how maleic acid can act as a versatile catalyst for biorefining, the concept of a biorefinery must first be understood. It is also important to understand how the chemistry and structure of substrates (corn kernels and corn stover) can influence chemical processing. The first section of this review describes some prominent biorefinery concepts. The second section discusses corn growth, harvest, structure, and chemistry, and how different corn products (kernels and stover) can be used in a biorefinery. Particular attention is paid to the chemistry of corn stover and current understanding of how corn stover structure impacts slurry properties. Additional literature review regarding chemicals significant to this work is included.

2.2 Biorefineries

The concept of a biorefinery is any facility that "processes biomass into a spectrum of bio-based products and bioenergy".[1] A petroleum refinery relies on the platform chemicals of benzene, toluene, xylenes, ethane, methane, and propylene to form the majority of petroleum-based products.[2] Similarly, a biorefinery needs to incorporate several platform chemicals to allow the production of a broad range of carbon-based products. **Figure 2.1** shows a generic biorefinery scheme, wherein biomass is converted to multiple value-added products in a synergistic refinery design. Werpy et al. identified 12 platform molecules, including furfural, 5-hydroxymethylfurfural, levulinic acid, and lactic acid[3] as promising platform molecules for a bio-based economy to replace a petroleum-based economy. Due to the wide range of refinery feedstocks and products, it is challenging to establish broadly accurate definitions of biorefinery parameters. In this review, a focus will be applied to refineries that use starch crops (corn kernels) and corn stover (agricultural residue) to produce hydroxymethylfurfural (HMF) or ethanol.

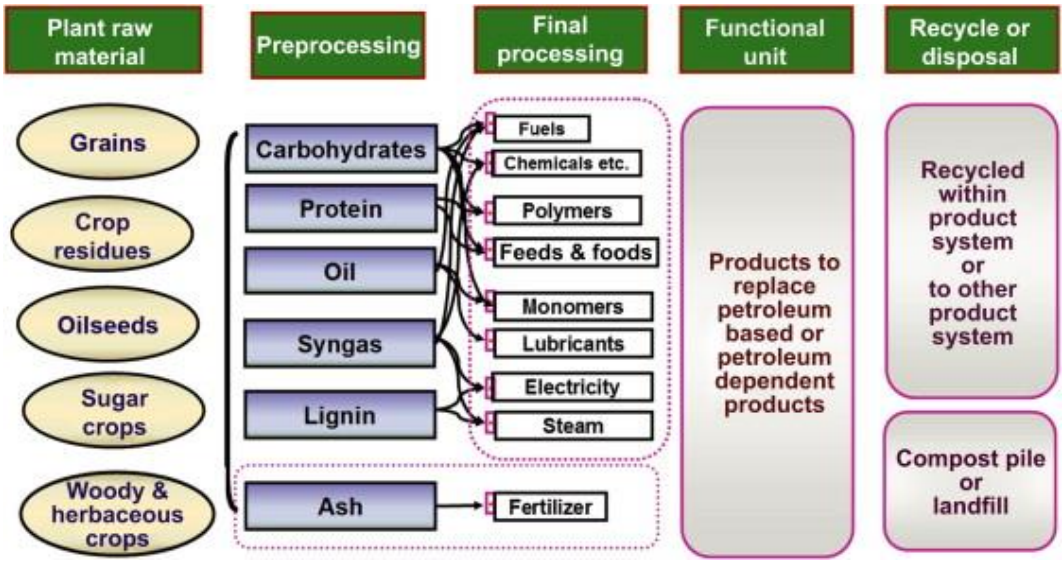

Figure 2.1. The bioeconomy A general flow diagram for the sourcing, production, and disposal of materials in a bio-based economy. Starches, oily, and herbaceous crops are processed into value-added products that displace petroleum-based products and can be recycled or composted.[4]

As with any industry, economic feasibility is the greatest driver of biorefinery design. To date, there are no second generation biorefineries that successfully operate at full capacity and produce a financial profit. While challenges with plant design that limit biorefinery feasibility will be discussed later in this chapter, another major challenge of biorefineries is substrate transport logistics. Several works demonstrate that the capital required to construct a 2nd generation ethanol refinery far exceeds the financial benefits of the facility.[5–7] This is caused in part due to the very low bulk density of materials such as corn stover. This drives up material transportation costs and limits the radius of material collection to 50 – 75 miles for a 2nd generation ethanol facility.[6] This means that biorefineries are unable to fully leverage economies of scale due to a limited substrate availability. Other strategies must be developed to help biorefineries take advantage of economies of scale through catalysts with different use and the use of multiple substrates for producing a versatile product portfolio.

2.3 Corn

2.3.1 Growth and harvest

Corn (*Zea mays*) is a starchy cereal grain that is a staple animal feed throughout the world. Of the total global production of corn (~1 billion tonnes per annum),[8] the majority of corn is used

for animal feed (39%), ethanol production (27%), and production of commodity starches and syrups (10%).[9] Corn plants typically grow to around 3 m in height and are composed of stalk, leaves, tassel, and ears, as shown in **Figure 2.2**.[10] During harvest by a combine, corn stalks are first cut a few inches above the ground and stalks and ears fall into the combine. A threshing drum then beats the corn to remove kernels from the corn cob. Kernels are able to fall through sieves and are collected. Material that does not pass through the sieves is ejected from the back of the machine. Ejected material, called corn stover, typically contains stalks, leaves, and cobs. Corn stover can be raked into rows and harvested into bales using swathers (windrowers) and balers, respectively.

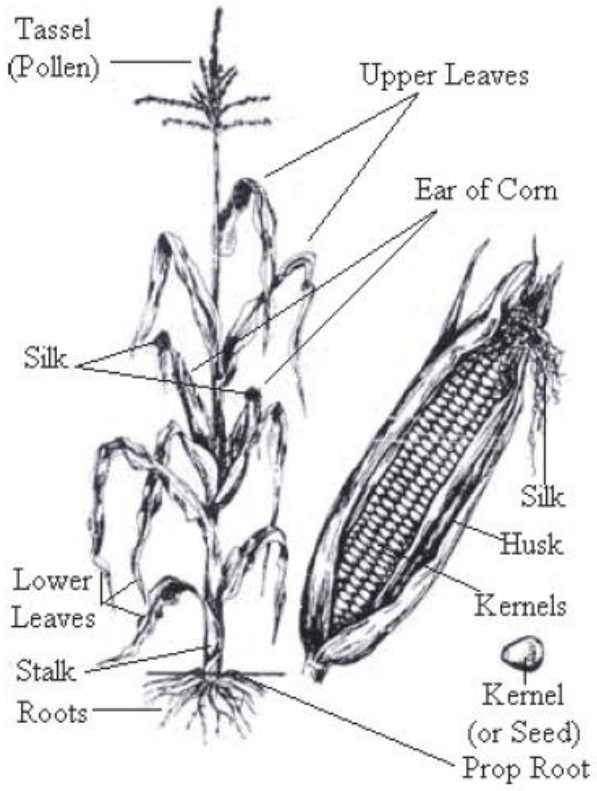

Figure 2.2. Corn Anatomy Anatomy of the corn plant and a corn ear.[10]

2.3.2 Corn Kernels

Corn kernels can be divided into four major anatomical regions. These are the endosperm, the pericarp, the germ, and the tip cap.[11] These account for 82%, 5%, 12%, and 1% of the kernel

mass, respectively.[11] The most common variety of corn grown for industrial agriculture is yellow dent corn.

Yellow dent corn is mostly composed of starch (61%), protein (8%), fiber (11%), oil (4%), and water (16%).[12] Through a process called wet-milling, corn fractions can be separated into separate streams of starch, germ (pericarp, tip cap, germ), fibers, and gluten (protein).[13] Oil can be extracted from corn germ and sold. Corn bran has uses as a high fiber feed and corn gluten is typically sold as an animal feed. The relatively pure starch stream can be sold as a food source or as a feedstock for other products.[13]

Corn starch is the primary energy source for the germination of corn embryos. Starch is a polymer of glucose monomers connected into chains of varying length by α-1,4 glycosidic bonds. Amylose and amylopectin are typical configurations of starch in corn. Amylose is a linear chain, while amylopectin is a highly-branched polymer with branches occurring every 24 – 30 molecules.[14,15] Branching chains are connected by α-1,6 linkages. **Figure 2.3** shows the structure of amylose and amylopectin. Yellow dent corn is considered a waxy variety of corn, containing ~99% amylopectin of the total starch content.[16]

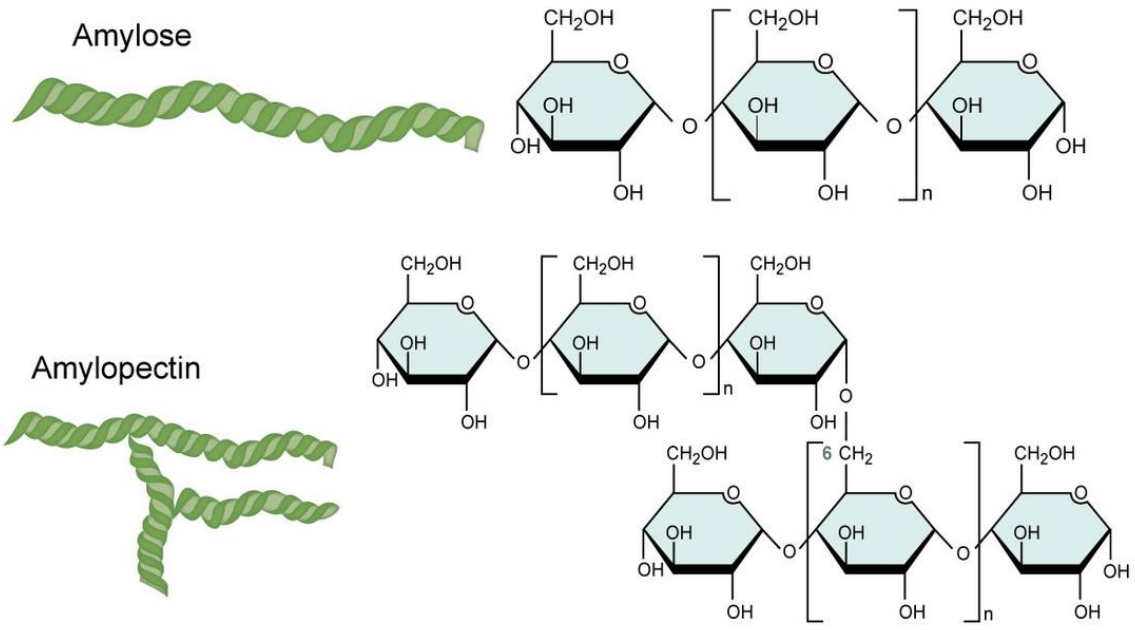

Figure 2.3. Starch Structures Structural differences in amylose (Straight-chains, top) and amylopectin (branched-chains, bottom) polymers of glucose commonly found in corn.[17]

2.3.3 Corn stover (Lignocellulosic material)

Corn stover is an agricultural residue left over from the harvest of corn grain and consists of leaves, stalks, cobs. Annual corn stover yields are around 120 million tons, corresponding to a potential ethanol production of 25 to 53 billion liters.[18] Corn stover consists of cellulose, hemicellulose, and lignin and is therefore considered a lignocellulosic biomass. As such, corn stover has garnered attention as a potential feedstock for 2nd generation ethanol production. The cellulose portion of corn stover is a polymer of repeating glucose monomers. Degradation of these polymers to monomeric glucose allows for the production of any number of chemicals by glucose-based fermentation or through other chemical transformations of glucose.[19]

Hemicellulose is an amorphous polymer composed of xylose, arabinose, glucose, and mannose in varying amounts.[20,21] Generally, xylose is the most represented monomer in hemicellulose. Some yeast can convert xylose to ethanol in addition to glucose, resulting in higher ethanol titers.[22] Other applications for hemicellulose-derived monomers involve the production of furans.[23] The third component of corn stover, lignin, is considered a major obstacle to transitioning to 2nd generation ethanol facilities. Lignin is a heteropolymer consisting of three main subunits: guaiacyl (G-unit), syringyl (S-unit), and hydroxyphenyl (H-unit).[24] These subunits are connected by a number of linkages and have a wide array of different side chains and chemical moieties that can be present. Plants incorporate lignin into their cell walls to add rigidity, structure, and protection to the plant.[25] These characteristics that make lignin favorable for viable plant growth also make lignocellulosic biomass very recalcitrant to degradation and conversion. Because of this, significant effort has been dedicated to developing technologies to remove the lignin sheath from around hemicellulose and cellulose, giving hydrolytic enzymes access to cellulose and increasing glucose yield. These treatments, generally called pretreatment and use elevated temperatures (>160 °C), can incorporate acids or bases to increase the degradation of lignin and hemicellulose.[26] While pretreatment is entirely necessary for good conversion of cellulose to glucose, recent modelling efforts have shown that solids loadings greater than 20% must be used in the pretreatment reactor to have an economically viable process.[5] Generally, the feasible technical limit for pretreatment solids loadings have been 10-15% due to the water binding capacity of lignocellulosic biomass reducing the free water content of the reactor.[27] With insufficient liquid in the reactor, the lignin matrix is not disrupted and pretreatment is ineffective.

2.4 Chemicals Significant to this Work

2.4.1 5-Hydroxymethylfurfural (HMF)

5-hydroxymethylfurfural (HMF) is a heterocyclic furan with both alcohol and aldehyde moieties and has a molecular mass of 126.11 g mole^{-1} **(Figure 2.4)**. HMF has a high capacity for chemical transformations and polymerizations due to its relative unsaturation and functional groups.[28] Because of this, HMF has been identified as a bio-product with significant potential to serve as a platform chemical **(Figure 2.5)**.[3]

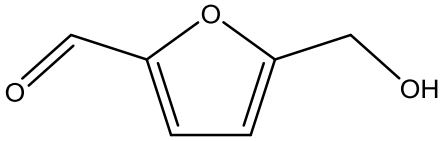

Figure 2.4. Structure of HMF

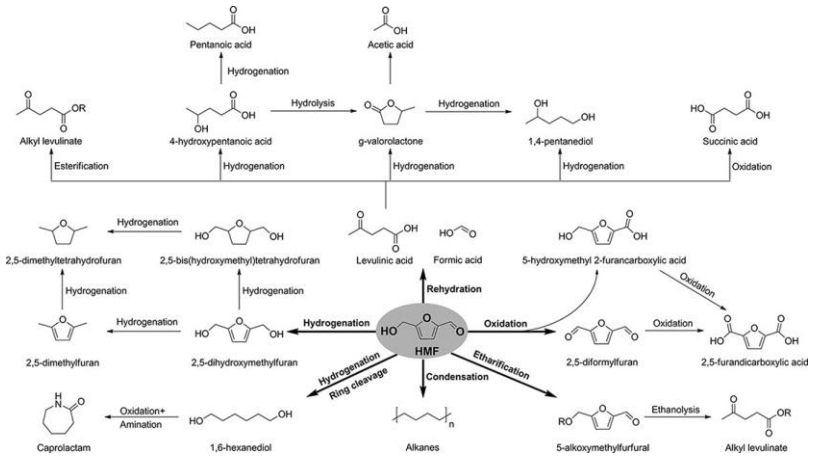

Figure 2.5. HMF as a platform chemical Some products that can be produced using HMF as a platform.[29]

Some notable chemicals that can be produced from HMF are:

- Levulinic acid (LVA): LVA is a ketone with a carboxylic acid group and is soluble in both water and polar solvents. LVA itself is a platform molecule that can be used for the production of the biofuel ethyl levulinate, a herbicide (aminolevulinic acid), a polymer building block (γ-valerolactone and 2-methyltetrahydrofuran).[30–32]

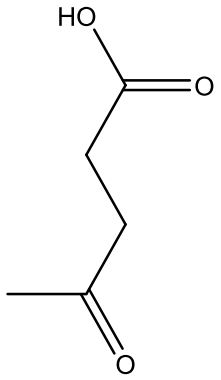

Figure 2.6. Structure of LVA

- Furandicarboxcylic acid (FDCA): FDCA is a furan-based chemical with carboxyl groups at the 2 and 5 carbons. FDCA can be used to replace terephthalic acid in the plastic polymer used to produce water bottles through polymerization with polyethylene.[33] A host of other potential polymerization reactions have been proposed for converting FDCA into nylon and tetrahydrofuran polymers with hopes of bio-plastics taking a share of global polymer markets.[34]

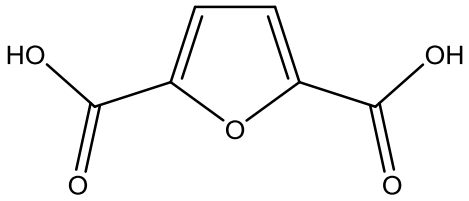

Figure 2.7. Structure of FDCA

- 2,5-furan dicarboxylic acid dimethyl ester (FDME): By using FDME rather than terephthalic acid, a new plastic (PTF) is produced, which has better gas barrier, weight, and strength characteristics than PET.[35] Since PTF is bio-based and has superior functionality compared to a similar petroleum-based product, companies have made significant investment into establishing FDME production facilities.[33] However, a major technical roadblock to the production of FDME is that current HMF production costs are too high.[36] Since terephthalic acid is so much cheaper than FDME, FDME has not yet experienced significant market growth. Producing low-cost HMF will increase the feasibility of FDME production and allow for PTF to be produced at costs competitive with PET.

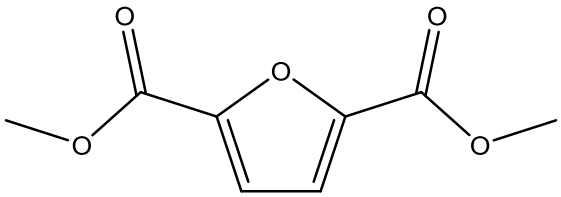

Figure 2.8. Structure of FDME

- 2,5-Dimethylfuran (DMF): DMF is a furanic product produced from fructose. It has an energy density 40% greater than that of ethanol and comparable to gasoline.36–38 Additionally, it is stable and water insoluble, making it a promising drop-in biofuel or bio-based fuel additive. Recent investigation has showed that DMF burns similarly to gasoline in a single cylinder engine.[37]

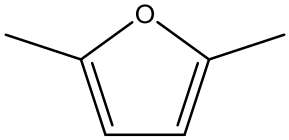

Figure 2.9. Structure of DMF

- Diformylfuran (DFF): DFF is a chemical intermediate for the production of numerous pharmaceuticals, pharmaceuticals, and ligands. DFF is produced through the oxidation of the hydroxyl moiety in HMF by Lewis bases and is a precursor to the formation of FDCA.[10,39,40]

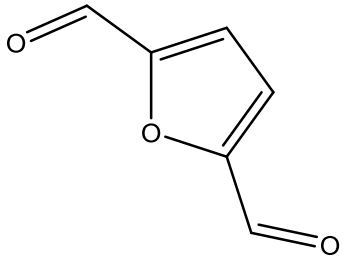

Figure 2.10. Structure of DFF

- Methyl-tetrahydrofuran (meTHF): meTHF is a highly flammable liquid frequently used as a replacement for tetrahydrofuran in applications where higher reaction temperatures or water immiscibility are required. A notable property is that meTHF decreases in water solubility as temperature increases.[41] This makes it a unique chemical with great potential for applications in biphasic reaction systems. meTHF can also act as a Lewis base in organometallic

reactions.[42] A major challenge with current meTHF in industry is relatively high costs. Creating cheaper HMF production processes could reduce the cost of meTHF and increase its use as a reaction solvent.

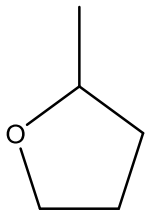

Figure 2.11. Structure of meTHF

- Alkanes: Bio-based n-hexane and n-pentane can be produced from glucose or fructose through HMF as a conversion intermediate.[43] Bio-based production of hexane has significant promise due to the widespread use of hexane as a solvent, fuel, and building block. Isomerization of hexane to branched hexanes improves a motor octane number.[44] Additionally, n-hexane can be used for the production of benzene, ethylene, and propylene through catalytic cracking.[45–47]

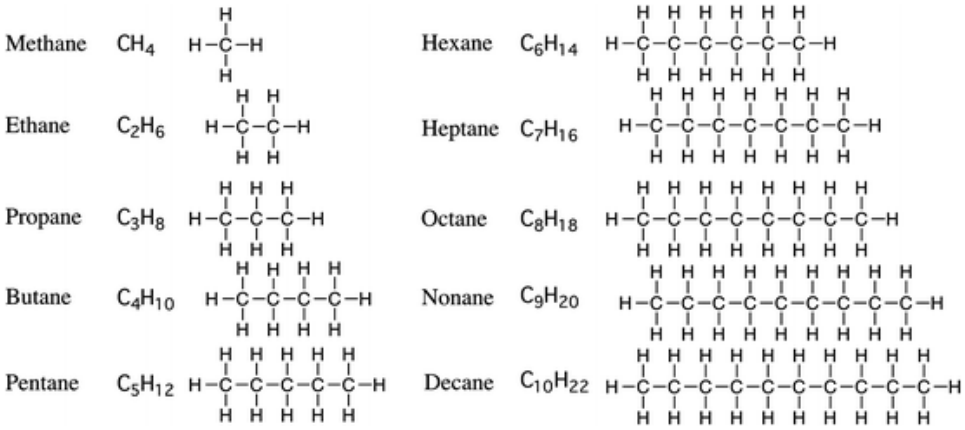

Figure 2.12. Alkanes Chemical structure of common alkanes[48]

Classically, HMF is synthesized through the dehydration of carbohydrates, especially fructose.[49,50] Brønsted acids such as hydrochloric acid or sulfuric acid can be used to catalyze this reaction.[51] A challenge with the production of HMF is the stability of HMF under reaction conditions.[49] Adding to this challenge, Brønsted acids are also able to catalyze the rehydration of HMF to LVA. Zhang et al., found that the activation energy of fructose conversion to HMF was higher than that of HMF to LVA.[52] This means that HMF yields were higher as reaction

temperature increased (at constant reaction time). The other major loss point of HMF yield is to humins. Humins are a broad identifier for 'lost' carbon in HMF production. Humins consist of polymers of fructose and HMF, HMF-HMF polymers, and HMF-LVA polymers[53,54] that continually grow under acidic conditions and eventually precipitate out of solution. Significant research has been dedicated to identifying means to reduce humin formation. The use of biphasic reactors has been fairly successful in overcoming humin formation, as HMF is extracted into an organic phase and away from Brønsted acids, reducing LVA and humin formation.[55–57] Biphasic reactors also facilitate downstream separations, however a roadblock to economic use of biphasic reactors for HMF production is that generally ratios of organic phase to aqueous phase are greater than 2:1, meaning that the capacity of the reactor is reduced to a third of a monophasic reactor. Another strategy to reduce humin formation is the use of cosolvents such as dimethylsulfoxide (DMSO) or acetone.[58–60] These polar, aprotic solvents are able to change how molecules interact with the aqueous reaction environment, but are unable to donate a proton or electron to the reaction. DMSO can also act as a water binder, preventing rehydration of HMF to LVA and increasing the rate of HMF dehydration. Many high yielding systems have been reported through the use of solvents. However, the use of fructose as a substrate creates a lower limit to HMF price that is greater than that of similar petroleum-derived chemicals (para xylene and terephthalic acid).[36] To overcome this limit, glucose is used as a substrate, requiring the addition of a Lewis acid to isomerize glucose to fructose. Recent work has shown that the balance between Lewis and Brønsted acids can limit HMF yield and selectivity.[61] This is a roadblock to economically viable production of HMF that has not yet been overcome.

2.4.2 Maleic acid

Maleic acid (cis-butenedioic acid) is a dicarboxylic acid with a molecular weight of 166.07 g mole^{-1} **(Figure 2.13).** Industrially, maleic acid is produced through hydrolysis of maleic anhydride, produced from benzene or butane (petroleum-derived).[62] Recent work has sought to produce maleic acid through the oxidation of furfural (bio-derived).[63–65] Maleic acid has been previously evaluated in the bioprocess industry for acid pretreatment of biomass and furfural production from biomass.[7,66,67] Notably, the addition of maleic acid drastically reduced the production of pretreatment byproducts produced from both cellobiose and other glucose polymers. In contrast, maleic acid readily catalyzed the degradation of biomass xylo-saccharides into

monomeric xylose, which was further dehydrated into furfural by maleic acid.[67,68] This process has potential for further integration into a maleic acid centered biorefinery, wherein a portion of the maleic acid required for processing is produced from furfural.

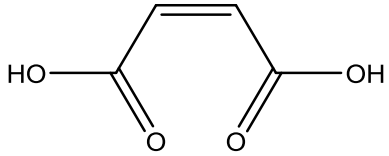

Figure 2.13. Structure of maleic acid

2.4.3 Aluminum Chloride ($AlCl_3$)

Aluminum chloride (aluminum trichloride, $AlCl_3$) is an inorganic, strong Lewis acid with a molecular weight of 133.34 g $mole^{-1}$. Aluminum chloride has been found to stabilize the opening of glucose rings to allow isomerization of glucose to fructose in the presence of maleic acid.[69,70] This occurs through coordination of Al^{3+} with two maleic acids and one glucose to form a transient complex for glucose ring opening and isomerization to fructose.[52,71]

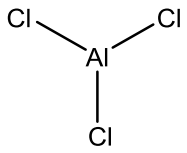

Figure 2.14. Structure of $AlCl_3$

2.4.4 Dimethylsulfoxide (DMSO)

Dimethylsulfoxide (DMSO) is a polar, aprotic solvent (does not donate a H^+ to solution) known for having a strong dehydrating capacity. Both polar and nonpolar compounds tend to be soluble in DMSO, and in turn, DMSO is generally miscible with most solvents.[72] The sulfur in DMSO can act as a nucleophile and the oxygen can act as an electrophile.[73] DMSO is considered non-toxic with a median lethal dose of 14.5 g kg^{-1}. For reference, the median lethal dose of ethanol is 7 g kg^{-1}. DMSO is not considered toxic for disposal in wastewater streams, however, the release of DMSO is limited since it is converted to dimethyl sulfide by anaerobic bacteria in water treatment, releasing a smell similar to rotting cabbage.[74]

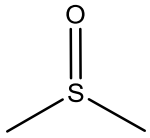

Figure 2.15. Structure of DMSO

2.4.5 Acetonitrile (ACN)

Acetonitrile (ACN) is a polar, aprotic solvent that is produced as a byproduct of acrylonitrile production.[75] It is generally considered a polar aprotic solvent and has numerous applications in organic synthesis and purifications.[76,77] ACN is miscible with water and many other organic solvents, however it is generally not soluble in saturated hydrocarbons.[77,78] An advantage of acetonitrile is the relatively low boiling point of 82.1 °C. Acetonitrile has a median lethal dose of 3 g kg^{-1}, considered to be moderately toxic and can be taken up through inhalation.[79] ACN is toxic due to enzymes which metabolize ACN to cyanide.[80] Because of this, safety considerations have to be made in a facility that uses large volumes of ACN.

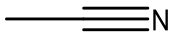

Figure 2.16. Structure of acetonitrile

2.4.6 Diethyl Ether/Ether (DEE)

DEE is the simplest organic ether and is a highly volatile chemical used to help combustion engines start and as a laboratory solvent. Ether has formerly been used as an intoxicant and general anesthetic. Ether is produced through the vapor phase dehydration of ethanol over alumina, sulfuric, or phosphoric acid catalysts.[81] DEE has very low solubility in water and as such, is used in liquid-liquid extraction of non-polar molecules from water.[82,83]

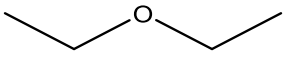

Figure 2.17. Structure of DEE

2.5 Techno-economic Analyses of Biorefineries

Techno-economic analysis (TEA) is a framework for evaluating the technical and economic feasibility of a proposed project.[84] In this framework, a process concept is defined and

a detailed mass and energy balance is performed using lab, pilot, predicted, or other available data sets. Using mass and energy balance results, as well as assumed costs of chemicals and power, an operating cost can be estimated. Additionally, the sizing and capital costing of equipment can be determined, and a discounted cash flow sheet can be created. By analyzing discounted cash flow as a function of varying inputs, a sensitivity analysis can be performed. Sensitivity analysis can be used to inform future research directions, identify potential scale-up challenges, and determine target production scales.

In the economic portion of the TEA, discounted cash flows are evaluated over a projected plant lifetime. A few critical values are used to evaluate the feasibility of an idea. These values are net present value (NPV), internal rate of return (IRR), and return on investment (ROI).[85] The NPV is the value of a future cashflow today, given a certain discount rate and can be used to fairly compare the worth of different future cashflows, over different time periods. In a sense, NPV normalizes different cashflows to a single value that can easily be compared. The IRR is similar to the NPV in that it allows for fair comparisons of different capital projects. IRR is defined as the discount rate at which the NPV of a series of cashflow is $0. ROI is a measure of the profitability of a project. A positive ROI suggests that a project will result in more economic benefits than costs. ROI is calculated as the ratio of the difference in NPV and capital cost to the capital cost, or profits earned over initial investment and is a widely-used financial metric.[85]

2.6 References

1. Biorefineries: Adding Value to the Sustainable Utilization of Biomass; 2009.
2. Nelson, W. L. Petroleum Refinery Engineering; 2018.
3. Program, B.; Werpy, T.; Petersen, G. Top Value Added Chemicals from Biomass Volume I-Results of Screening for Potential Candidates from Sugars and Synthesis Gas Produced by the Staff at Pacific Northwest National Laboratory (PNNL) National Renewable Energy Laboratory (NREL) Office of Biomass Program (EERE) For the Office of the Energy Efficiency and Renewable Energy.
4. Gavrilescu, M. Biorefinery Systems: An Overview. In Bioenergy Research: Advances and Applications; 2014; pp 219–241.
5. Humbird, D.; Mohagheghi, A.; Dowe, N.; Schell, D. J. Economic Impact of Total Solids Loading on Enzymatic Hydrolysis of Dilute Acid Pretreated Corn Stover. Biotechnol. Prog. 2010, 26 (5), 1245–1251. https://doi.org/10.1002/btpr.441.

6. Carolan, J. E.; Joshi, S. V.; Dale, B. E. Technical and Financial Feasibility Analysis of Distributed Bioprocessing Using Regional Biomass Pre-Processing Centers. J. Agric. Food Ind. Organ. 2007, 5 (2). https://doi.org/10.2202/1542-0485.1203.

7. Tao, L.; Aden, A.; Elander, R. T.; Pallapolu, V. R.; Lee, Y. Y.; Garlock, R. J.; Balan, V.; Dale, B. E.; Kim, Y.; Mosier, N. S.; et al. Process and Technoeconomic Analysis of Leading Pretreatment Technologies for Lignocellulosic Ethanol Production Using Switchgrass. Bioresour. Technol. 2011, 102 (24), 11105–11114. https://doi.org/10.1016/j.biortech.2011.07.051.

8. Approved by the World Agricultural Outlook Board World Agricultural Production; 2019.

9. Iowa Corngrowers Association.

10. Halliday, G. A.; Young, R. J.; Grushin, V. V. One-Pot, Two-Step, Practical Catalytic Synthesis of 2,5-Diformylfuran from Fructose. Org. Lett. 2003, 5 (11), 2003–2005. https://doi.org/10.1021/ol034572a.

11. Hossain, A. Dry and Wet Milling of Corn; 2013.

12. Clifford, C. Composition of Corn and Yield of Ethanol from Corn https://www.e-education.psu.edu/egee439/node/672 (accessed Dec 11, 2019).

13. Arora, A.; Niu, Y.; Tumbleson, M. E.; Rausch, K. D. Laboratory Wet Milling of Corn: Milling Fraction Correlations and Variations among Crop Years. Cereal Chem. 2008, 85 (2), 207–210. https://doi.org/10.1094/CCHEM-85-2-0207.

14. Takeda, Y.; Maruta, N.; Hizukuri, S. Structures of Amylose Subfractions with Different Molecular Sizes; 1992; Vol. 226.

15. Hizukuri, F. Relationship between the distribution of the chain length of amylopectin and the crystalline structure of starch granules; 1985; Vol. 141.

16. Cowieson, A. J.; Vieira, S. L.; Stefanello, C. Exogenous Microbial Amylase in the Diets of Poultry: What Do We Know? J. Appl. Poult. Res. 2019, 28 (3), 556–565. https://doi.org/10.3382/japr/pfy044.

17. Sanyang, M. L.; Ilyas, R. A.; Sapuan, S. M.; Jumaidin, R. Sugar Palm Starch-Based Composites for Packaging Applications. In Bionanocomposites for Packaging Applications; Springer International Publishing, 2017; pp 125–147. https://doi.org/10.1007/978-3-319-67319-6_7.

18. Young, M.; Boland, M.; Hofstrand, D. Current Issues in Ethanol Production. Value Mark. Resour. Cent. 2007.

19. Blanch, H. W.; Wilke, C. R. Sugars and chemicals from cellulose 1. Introduction 72 2. Sources and Structure of Cellulose 73 2.1. Cellulose Sources 73 2.2. Structure and Morphology of Cellulose 75 3. Enzymatic Hydrolysis of Cellulose 78 3.1. The Cellulase Enzyme System 78 3.2. Production of Cellulase Enzymes 82 3.3. Hydrolysis of Cellulosic Materials 86.

20. Darvill, J. E.; Mcneil, M.; Darvill, A. G.; Albersheim2, P. Structure of Plant Cell Walls XI. Glucuronoarabinoxylan, a second hemicellulose in the primary cell walls of suspension-cultured sycamore cells'; 1980; Vol. 66.

21. Bauer, W. D.; Talmadge, K. W.; Keegstra, K.; Albersheim°, P. The Structure of Plant Cell Walls II. The hemicellulose of the walls of suspension-cultured sycamore cells'; 1973; Vol. 51.

22. Ho, N. W. Y.; Chen, Z.; Brainard, A. P. Genetically Engineered Saccharomyces Yeast Capable of Effective Cofermentation of Glucose and Xylose; 1998; Vol. 64.

23. Kim, E. S.; Liu, S.; Abu-Omar, M. M.; Mosier, N. S. Selective Conversion of Biomass Hemicellulose to Furfural Using Maleic Acid with Microwave Heating. Energy and Fuels 2012, 26 (2), 1298–1304. Https://doi.org/10.1021/ef2014106.

24. Kaplan, D. L. Biopolymers from Renewable Resources, 1st ed.; Springer: Heidelberg, 1998. Https://doi.org/https://doi.org/10.1007/978-3-662-03680-8.

25. Pedersen, J. F.; Vogel, K. P.; Funnell, D. L. Impact of Reduced Lignin on Plant Fitness. In Symposium Lignin and Forage Digestibility; 2005; pp 812–819.

26. Hsu, T. A.; Ladisch, M. R.; Tsao, G. T. Alcohol from Cellulose. Chem. Technol. 1980, 10, 315–319.

27. Cheng, Y. S.; Zheng, Y.; Yu, C. W.; Dooley, T. M.; Jenkins, B. M.; Vandergheynst, J. S. Evaluation of High Solids Alkaline Pretreatment of Rice Straw. Appl. Biochem. Biotechnol. 2010, 162 (6), 1768–1784. https://doi.org/10.1007/s12010-010-8958-4.

28. Wang, T.; Nolte, M. W.; Shanks, B. H. Catalytic Dehydration of C6 Carbohydrates for the Production of Hydroxymethylfurfural (HMF) as a Versatile Platform Chemical. Green Chemistry. February 2014, pp 548–572. https://doi.org/10.1039/c3gc41365a.

29. Bhaumik, P.; Dhepe, P. L. Solid Acid Catalyzed Synthesis of Furans from Carbohydrates. Catal. Rev. - Sci. Eng. 2016, 58 (1), 36–112. https://doi.org/10.1080/01614940.2015.1099894.

30. Bozell, J. J.; Moens, L.; Elliott, D. C.; Wang, Y.; Neuenscwander, G. G.; Fitzpatrick, S. W.; Bilski, R. J.; Jarnefeld, J. L. Production of Levulinic Acid and Use as a Platform Chemical for Derived Products; 2000; Vol. 28.

31. Lange, J. P.; Vestering, J. Z.; Haan, R. J. Towards "bio-Based" Nylon: Conversion of γ-Valerolactone to Methyl Pentanoate under Catalytic Distillation Conditions. Chem. Commun. 2007, No. 33, 3488–3490. https://doi.org/10.1039/b705782b.

32. Manzer, L. E. Catalytic Synthesis of α-Methylene-γ-Valerolactone: A Biomass-Derived Acrylic Monomer. Appl. Catal. A Gen. 2004, 272 (1–2), 249–256. https://doi.org/10.1016/j.apcata.2004.05.048.

33. DuPont_download_card_339_9f180f605b462668633962c6aa82e157.

34. Rosatella, A. A.; Simeonov, S. P.; Frade, R. F. M.; Afonso, C. A. M. 5-Hydroxymethylfurfural (HMF) as a Building Block Platform: Biological Properties, Synthesis and Synthetic Applications. Green Chemistry. April 2011, pp 754–793. https://doi.org/10.1039/c0gc00401d.

35. Van der Hoeven, D. More biobased plastics for bottles: Dupont announces PTF https://www.biobasedpress.eu/2016/02/more-biobased-plastics-for-bottles-dupont-announces-ptf/.

36. Kazi, F. K.; Patel, A. D.; Serrano-Ruiz, J. C.; Dumesic, J. A.; Anex, R. P. Techno-Economic Analysis of Dimethylfuran (DMF) and Hydroxymethylfurfural (HMF) Production from Pure Fructose in Catalytic Processes. Chem. Eng. J. 2011, 169 (1–3), 329–338. https://doi.org/10.1016/j.cej.2011.03.018.

37. Zhong, S.; Daniel, R.; Xu, H.; Zhang, J.; Turner, D.; Wyszynski, M. L.; Richards, P. Combustion and Emissions of 2,5-Dimethylfuran in a Direct-Injection Spark-Ignition Engine. Energy and Fuels 2010, 24 (5), 2891–2899. https://doi.org/10.1021/ef901575a.

38. Román-Leshkov, Y.; Barrett, C. J.; Liu, Z. Y.; Dumesic, J. A. Production of Dimethylfuran for Liquid Fuels from Biomass-Derived Carbohydrates. Nature 2007, 447 (7147), 982–985. https://doi.org/10.1038/nature05923.

39. Ma, J.; Du, Z.; Xu, J.; Chu, Q.; Pang, Y. Efficient Aerobic Oxidation of 5-Hydroxymethylfurfural to 2,5-Diformylfuran, and Synthesis of a Fluorescent Material. ChemSusChem 2011, 4 (1), 51–54. https://doi.org/10.1002/cssc.201000273.

40. Amarasekara, A. S.; Green, D.; Williams, L. T. D. Renewable Resources Based Polymers: Synthesis and Characterization of 2,5-Diformylfuran-Urea Resin. Eur. Polym. J. 2009, 45 (2), 595–598. https://doi.org/10.1016/j.eurpolymj.2008.11.012.

41. Pace, V.; Hoyos, P.; Castoldi, L.; Domínguez De María, P.; Alcántara, A. R. 2-Methyltetrahydrofuran (2-MeTHF): A Biomass-Derived Solvent with Broad Application in Organic Chemistry. ChemSusChem. Wiley-VCH Verlag 2012, pp 1369–1379.

42. Aycock, D. F. Solvent Applications of 2-Methyltetrahydrofuran in Organometallic and Biphasic Reactions. Org. Process Res. Dev. 2007, 11 (1), 156–159. https://doi.org/10.1021/op060155c.

43. West, R. M.; Liu, Z. Y.; Peter, M.; Dumesic, J. A. Liquid Alkanes with Targeted Molecular Weights from Biomass-Derived Carbohydrates. ChemSusChem 2008, 1 (5), 417–424. https://doi.org/10.1002/cssc.200800001.

44. Chica, A.; Corma, A. Hydroisomerization of Pentane, Hexane, and Heptane for Improving the Octane Number of Gasoline; 1999; Vol. 187.

45. Post, J. G.; Van Hooff, J. H. C. Acidity and Activity of H-ZSM-5 Measured with NHa-t.p.d. and n-Hexane Cracking.

46. Konno, H.; Okamura, T.; Kawahara, T.; Nakasaka, Y.; Tago, T.; Masuda, T. Kinetics of N-Hexane Cracking over ZSM-5 Zeolites - Effect of Crystal Size on Effectiveness Factor and Catalyst Lifetime. Chem. Eng. J. 2012, 207–208, 490–496. https://doi.org/10.1016/j.cej.2012.06.157.

47. Babitz, S. M.; Williams, B. A.; Miller, J. T.; Snurr, R. Q.; Haag, W. O.; Kung, H. H. Monomolecular Cracking of N-Hexane on Y, MOR, and ZSM-5 Zeolites.

48. Vancik, H. Alkanes, Composition, Constitution, and Configuration. In Organic Chemistry for the Life Sciences; 2014.

49. Kuster, B. F. M. 5-Hydroxymethylfurfural (HMF). A Review Focussing on Its Manufacture*.

50. Van Dam, H. E.; Kieboom, A. P. G.; Van Bekkum, H. The Conversion of Fructose and Glucose in Acidic Media: Formation of HydroxymethylfurFuraI.

51. Szmant, H. H.; Chundury, D. D. The Preparation of 5-Hydroxymethylfurfuraldehyde from High Fructose Corn Syrup and Other Carbohydrates; 1981; Vol. 31.

52. Zhang, X.; Murria, P.; Jiang, Y.; Xiao, W.; Kenttämaa, H. I.; Abu-Omar, M. M.; Mosier, N. S. Maleic Acid and Aluminum Chloride Catalyzed Conversion of Glucose to 5-(Hydroxymethyl) Furfural and Levulinic Acid in Aqueous Media. Green Chem. 2016, 18 (19), 5219–5229. https://doi.org/10.1039/c6gc01395c.

53. Tsilomelekis, G.; Orella, M. J.; Lin, Z.; Cheng, Z.; Zheng, W.; Nikolakis, V.; Vlachos, D. G. Molecular Structure, Morphology and Growth Mechanisms and Rates of 5- (HMF) Derived Humins. Green Chem. 2016, 18 (7), 1983–1993.

54. Van Zandvoort, I.; Koers, E. J.; Weingarth, M.; Bruijnincx, P. C. A.; Baldus, M.; Weckhuysen, B. M. Structural Characterization of 13C-Enriched Humins and Alkali-Treated 13C Humins by 2D Solid-State NMR. Green Chem. 2015, 17 (8), 4383–4392.

55. Román-Leshkov, Y.; Dumesic, J. A. Solvent Effects on Fructose Dehydration to 5-Hydroxymethylfurfural in Biphasic Systems Saturated with Inorganic Salts. Top. Catal. 2009, 52 (3), 297–303. https://doi.org/10.1007/s11244-008-9166-0.

56. Okano, T.; Qiao, K.; Bao, Q.; Tomida, D.; Hagiwara, H.; Yokoyama, C. Dehydration of Fructose to 5-Hydroxymethylfurfural (HMF) in an Aqueous Acetonitrile Biphasic System in the Presence of Acidic Ionic Liquids. Appl. Catal. A Gen. 2013, 451, 1–5.

57. Yang, Y.; Du, Z.; Ma, J.; Lu, F.; Zhang, J.; Xu, J. Biphasic Catalytic Conversion of Fructose by Continuous Hydrogenation of HMF over a Hydrophobic Ruthenium Catalyst. ChemSusChem 2014, 7 (5), 1352–1356. https://doi.org/10.1002/cssc.201301270.

58. Wang, H.; Kong, Q.; Wang, Y.; Deng, T.; Chen, C.; Hou, X.; Zhu, Y. Graphene Oxide Catalyzed Dehydration of Fructose into 5- Hydroxymethylfurfural with Isopropanol as Cosolvent. ChemCatChem 2014, 6 (3), 728–732. https://doi.org/10.1002/cctc.201301067.

59. Weingarten, R.; Rodriguez-Beuerman, A.; Cao, F.; Luterbacher, J. S.; Alonso, D. M.; Dumesic, J. A.; Huber, G. W. Selective Conversion of Cellulose to Hydroxymethylfurfural in Polar Aprotic Solvents. ChemCatChem 2014, 6 (8), 2229–2234. https://doi.org/10.1002/cctc.201402299.

60. Román-Leshkov, Y.; Chheda, J. N.; Dumesic, J. A. Phase Modifiers Promote Efficient Production of HMF from Fructose. Science (80-.). 2006, 312, 1933–1937.

61. Choudhary, V.; Mushrif, S. H.; Ho, C.; Anderko, A.; Nikolakis, V.; Marinkovic, N. S.; Frenkel, A. I.; Sandler, S. I.; Vlachos, D. G. Insights into the Interplay of Lewis and Brønsted Acid Catalysts in Glucose and Fructose Conversion to 5-(Hydroxymethyl)Furfural and Levulinic Acid in Aqueous Media. J. Am. Chem. Soc. 2013, 135 (10), 3997–4006. https://doi.org/10.1021/ja3122763.

62. Van Nostrand. Maleic anhydride, maleic acid, and fumaric acid. 2006. Van Nostrand's Scientific Encylopedia.

63. Shi, S.; Guo, H.; Yin, G. Synthesis of Maleic Acid from Renewable Resources: Catalytic Oxidation of Furfural in Liquid Media with Dioxygen. Catal. Commun. 2011, 12 (8), 731–733. https://doi.org/10.1016/j.catcom.2010.12.033.

64. Guo, H.; Yin, G. Catalytic Aerobic Oxidation of Renewable Furfural with Phosphomolybdic Acid Catalyst: An Alternative Route to Maleic Acid. J. Phys. Chem. C 2011, 115 (35), 17516–17522. https://doi.org/10.1021/jp2054712.

65. Alonso-Fagúndez, N.; Agirrezabal-Telleria, I.; Arias, P. L.; Fierro, J. L. G.; Mariscal, R.; Granados, M. L. Aqueous-Phase Catalytic Oxidation of Furfural with H2O2: High Yield of Maleic Acid by Using Titanium Silicalite-1. RSC Adv. 2014, 4 (98), 54960–54972. https://doi.org/10.1039/c4ra11563e.

66. Mosier, N. S.; Sarikaya, A.; Ladisch, C. M.; Ladisch, M. R. Characterization of Dicarboxylic Acids for Cellulose Hydrolysis. Biotechnol. Prog. 2001, 17 (3), 474–480. https://doi.org/10.1021/bp010028u.

67. Lu, Y.; Mosier, N. S. Biomimetic Catalysis for Hemicellulose Hydrolysis in Corn Stover. In Biotechnology Progress; 2007; Vol. 23, pp 116–123.

68. Lu, Y.; Mosier, N. S. Kinetic Modeling Analysis of Maleic Acid-Catalyzed Hemicellulose Hydrolysis in Corn Stover. Biotechnol. Bioeng. 2008, 101 (6), 1170–1181.

69. Zhang, X.; Hewetson, B. B.; Mosier, N. S. Kinetics of Maleic Acid and Aluminum Chloride Catalyzed Dehydration and Degradation of Glucose. Energy and Fuels 2015, 29 (4), 2387–2393. https://doi.org/10.1021/ef502461s.

70. Yang, Y.; Hu, C.; Abu-Omar, M. M. Conversion of Glucose into Furans in the Presence of AlCl 3 in an Ethanol-Water Solvent System. Bioresour. Technol. 2012, 116, 190–194. https://doi.org/10.1016/j.biortech.2012.03.126.

71. Tang, J.; Guo, X.; Zhu, L.; Hu, C. Mechanistic Study of Glucose-to-Fructose Isomerization in Water Catalyzed by [Al(OH)2(Aq)]+. ACS Catal. 2015, 5 (9),

72. D. Martin, H.; Weise, C. A.; Niclas, H. J. The Solvent Dimethylsulfoxide. Angew. Chemie 1967, 6 (4).

73. Chebolu, R.; Bahuguna, A.; Sharma, R.; Mishra, V. K.; Ravikumar, P. C. An Unusual Chemoselective Oxidation Strategy by an Unprecedented Exploration of an Electrophilic Center of DMSO: A New Facet to Classical DMSO Oxidation. Chem. Commun. 2015, 51 (84), 15438–15441. https://doi.org/10.1039/c5cc05713b.

74. Dimethyl Sulphoxide Reduction by Micro-Organisms; 1978; Vol. 105.

75. Blackford1, D. S.; York, R. Vapor-Liquid Equilibria of the System Acrylonitrile-Acetonitrile-Water The Total Pressure over the Boiling Mixtures Was Main-Tained at 760 Mm. of Hg Absolute by Means of a Cartesian.

76. Nyquist, R. A. Solvent-Induced Nitrile Frequency Shifts: Acetonitrile and Benzonitrile; 1990.

77. Walter, M.; Ramaley, L.; Coetzee, J. F.; Cunningham, G. P.; McGuire, D. K.; Forcier, G. A.; Oliver, J. W.; Sherman, E. O.; Olson, D. C. Purification of ACN; 1962; Vol. 34.

78. Locke, D. C. Chromatographic study of solutions acetonitrile of hydrocarbons in an investigation of the Mammalian Toxicity 1993.

79. Geller, R. J.; Ekins, B. R.; Iknoian, R. C. Cyanide Toxicity From Acetonitrile-Containing False Nail Remover; 1991.

80. Varisli, D.; Dogu, T.; Dogu, G. Ethylene and Diethyl-Ether Production by Dehydration Reaction of Ethanol over Different Heteropolyacid Catalysts. Chem. Eng. Sci. 2007, 62 (18–20), 5349–5352. https://doi.org/10.1016/j.ces.2007.01.017.

81. Kralj, J. G.; Sahoo, H. R.; Jensen, K. F. Integrated Continuous Microfluidic Liquid-Liquid Extraction. Lab Chip 2007, 7 (2), 256–263. https://doi.org/10.1039/b610888a.

82. Gan, S. H.; Ismail, R.; Adnan, W. A. W.; Wan, Z. Method Development and Validation of a High-Performance Liquid Chromatographic Method for Tramadol in Human Plasma Using Liquid-Liquid Extraction; 2002.

83. Sharif, M. N. Technology and Economics Basis for Techno-Economic Policy Analysis 2011

84. Boardman, A.; Greenberg, D.; Vining, A.; Weimer, D. Cost Benefit Analysis; Pearson, 2010.

3. MOLECULAR DYNAMIC SIMULATIONS AND EXPERIMENTAL VERIFICATION TO DETERMINE MECHANISM OF CO-SOLVENTS ON INCREASED HMF YIELDS FROM GLUCOSE

The contents of Chapter 3 are adapted from the journal article "Molecular dynamic simulations and experimental verification to determine mechanism of co-solvents on increased HMF yields from glucose", a published manuscript in the Journal *ACS Sustainable Chemistry and Engineering*.

3.1 Introduction

Photosynthetically-derived carbohydrates are a promising platform for producing fuels and chemicals with improved functionality over petroleum-based products and will facilitate a reduction in the petroleum required for commodity chemical production.[1–3] In a well-established industrial process, these carbohydrates can be obtained from starch through the process of hydrolysis to glucose. Corn-derived glucose is a promising candidate to produce low-carbon fuels and chemicals and warrants further research and development as a production platform for commodity chemicals and fuels.[4–6]

One of these valuable platform chemicals is 5-hydroxymethylfurfural (HMF), which can be used to produce plastics, adhesives, fuels, and pharmaceuticals.[7–12] One of the notable products that can be produced from HMF is 2,5-furandicarboxylic acid (FDCA), which can replace terephthalic acid in the production of poly(ethylene terephthalate) (PET), which becomes poly(ethylene 2,5-furandicarboxylate) (PEF) when FDCA is used in place of terephthalic acid.[13] In addition to being renewably sourced, PEF is also more lightweight and has better gas barrier properties than PET, making it a promising sustainable plastic for food and beverage packaging applications.[14]

The majority of previously described processes for the production of HMF from renewable sources focus on dehydration of bio-derived fructose.[12] Since fructose is typically produced from glucose, using glucose to directly produce HMF would lead to more economical processes by bypassing production of fructose in a separate reaction.[15] However, Brønsted acids do not readily catalyze the conversion of glucose to HMF since glucose tends to exist as a six member ring rather than a five member ring.[16] Because of this, glucose must first be isomerized to fructose, which is then dehydrated to HMF. Lewis acids, such as aluminum chloride ($AlCl_3$), have been shown to

catalyze the isomerization of glucose to fructose.[17–19] Fructose can then be dehydrated to HMF in the same reactor by the addition of Brønsted acids such as maleic acid and hydrochloric acid (HCl). Maleic acid was found to have two times greater selectivity for HMF and levulinic acid (LVA) production in combination with $AlCl_3$ than HCl combined with $AlCl_3$.[17] Reduced formation of humins was caused in part by the stabilization of the acyclic form of glucose in the presence of maleic acid.[20] However, maleic acid and $AlCl_3$ reactions consumed less than 80% of available glucose, while HCl combined with $AlCl_3$ consumed all available glucose within 6 minutes at 180 °C.[17] Increasing the rate and extent of glucose disappearance during HMF production by maleic acid and $AlCl_3$, while maintaining high selectivity, would lead to higher HMF titers and more economically viable commercial processes.

Polar, aprotic solvents such as dimethylsulfoxide (DMSO), acetonitrile, acetone, and sulfolane have been shown to increase HMF yield and selectivity from sugar.[21–24] While the increase in HMF yield is well-studied in aprotic solvents, few studies have been conducted regarding how these solvents fundamentally affect the kinetics of HMF production. By studying how kinetics are altered in the presence of polar, aprotic solvents, it is hypothesized that strategies can be developed to increase HMF yield, increase rate of production, and reduce humin formation.

Here, we report the reaction kinetics of HMF production from glucose in polar aprotic solvent/water mixtures using maleic acid combined with aluminum chloride. Notably, the addition of 20% (v/v) DMSO to water more than doubles the rate of fructose dehydration to HMF. In addition, reactions in 40% (v/v) acetonitrile doubles the rate of glucose isomerization to fructose. Molecular dynamics simulations suggest that changes in the hydration shell around glucose may account for these observations. We demonstrate that a reaction media mixture of water, DMSO, and acetonitrile greatly increases HMF yields from glucose at industrially relevant substrate concentrations (30 wt.%).

3.2 Methodology

3.2.1 Substrates and reactors

Glucose, fructose, levulinic acid (LVA), HMF, maleic acid, $AlCl_3$, acetonitrile, and DMSO were all purchased form Sigma-Aldrich (St. Louis, MO, USA). Stainless steel reactors for conducting reactions were used as described in previous works.[17] Briefly, reactions were

performed in 316L stainless steel tubing (8 mm diameter, 2.1 mm wall thickness, 70 mm length) and fitted with 1.2 cm Swagelok end fittings (Swagelok, Solon, OH, USA). Reactors had a volume of ~3.5 mL and were filled with 2 mL of reaction solution, allowing for gas and liquid expansion within the reactor.

3.2.2 Reaction procedures

For kinetic analysis, reactions were performed at temperatures of 120, 140, and 160 °C using glucose (250 mM), fructose (250 mM), and HMF (60 mM) separately as substrates to allow determination of individual reaction rates. Reaction solution (2 mL) was placed in the stainless steel reactor and the reactor was sealed tightly. Reactors were then immersed in a sand bath for the desired reaction time, with an additional two minutes of heat-up.[17] Immediately after the reaction time ended, reactors were removed from the sand bath and immersed in cool water. Reaction solution was then filtered through a 0.2 μm nylon filter and diluted for high pressure liquid chromatography (HPLC). HPLC was performed on an HPX-87H AMINEX column (BioRad, Hercules, CA, USA) with a mobile phase of 10 mM H_2SO_4 in water and 5% (w/w) acetonitrile. Acetonitrile and an increased H_2SO_4 concentration were used to facilitate the separation of glucose from maleic acid and fructose from malic acid.[20] The flow rate through the Waters 1525 pump and Waters 2412 Refractive Index Detector (Waters Corp. Milford, MA, USA) was 0.6 mL per minute with a column temperature of 65 °C. The concentration of all reactants and products was determined by external calibration standards. For reactions with 30 wt. % glucose, 0.6 g of glucose was first placed in the reactor tube. Reaction solution with the desired catalyst and cosolvent concentration was then added to bring the total mass added to the reactor to 2 g. Dilutions for these reactions were performed on a weight basis, since it could no longer be assumed that the density of the reaction solution was that of water to allow for volumetric dilutions. Samples were diluted 40-50x, to ensure that all components were less than 2 g/L for HPLC analysis. After this dilution was performed, it was assumed that the density of this solution was equal to the density of water for calculating the mass of solute present.

3.2.3 Molecular dynamic simulations

All molecular dynamics (MD) simulations were performed using GROMACS (version 2016.5) package.25 The simulation systems consisted of glucose in water and in acetonitrile-water mixtures at the same concentrations as in kinetic experiments. Details of system size are listed in the **Table 3.1.** OPLS-AA force field was used for glucose[26] and acetonitrile[27] and two different water models (TIP3P and TIP4P)[28] were employed for water. Pothoczki et al. demonstrated the MD simulation of acetonitrile using OPLS-AA model provided a good agreement with experimental data, such as scattering structure factors.[29] In all simulations, periodic boundary conditions were applied in all directions. The bonds with H-atoms were constrained to their equilibrium lengths with LINCS algorithm[30] and a 1 fs time step was used. A short-range cutoff of 1.2 nm was used for van der Waals interactions; long-range electrostatic interactions were treated with Particle Mesh Ewald method.[31] Prior to production simulations, systems were energy minimized for 5000 steps and equilibrated at 300 K for 2 ns in NVT ensemble. Production runs were carried out for 100 ns using the velocity-rescaling thermostat[32] to maintain temperature at 300 K, and the Parrinello-Rahman barostat to maintain pressure at 1 atm.[33] The final 20 ns trajectory was used for data analysis using tools available in GROMACS and simulations were visualized with VMD.[34]

Table 3.1. MD Simulation Conditions Operating conditions used for molecular dynamic simulations

Systems	# of glucose molecules	# of water molecules	# of acetonitrile molecules
Water	20	4149	0
20 % acetonitrile: water	20	3334	290
40 % acetonitrile: water	20	2563	580

3.2.4 Kinetic modeling

It was first assumed that all reactors were well mixed and completely isothermal during reactions after heat-up. A system of differential equations were derived using a monophasic model assuming first order reaction kinetics, as shown in **Scheme 3.1 and Equations 3.1 – 3.4** as previously described by Zhang et al.[17] In this reaction, glucose is isomerized by Al^{3+} to fructose.

$$\frac{d[\text{Glucose}]}{dt} = -(k_1 + k_4)[\text{Glucose}] + k_{-1}[\text{Fructose}] \quad (3.1)$$

$$\frac{d[Fructose]}{dt} = -(k_2 + k_5)[Fructose] + k_1[Glucose] \quad (3.2)$$

$$\frac{d[HMF]}{dt} = -(k_3 + k_6)[HMF] + k_2[Fructose] \quad (3.3)$$

$$\frac{d[LVA]}{dt} = k_3[HMF] \quad (3.4)$$

Fructose is subsequently dehydrated to HMF, which can be partially rehydrated to LVA. Each reaction step can also result in the formation of insoluble humins and degradation products. Each rate was estimated using linear regression in Microsoft Excel. For each substrate, data points were only used if the substrate concentration was greater than 75% of the initial substrate concentration, to obtain only initial reaction rates and rule out effects of secondary reactions. A minimum of three time points, with duplicate reactions, were used for each rate regression. At reaction temperatures not evaluated during development of the model, kinetic rates were predicted by the Arrhenius equation using experimentally determined activation energies and kinetic rates measured at 120 °C as a reference temperature. MATLAB was used to simulate reactions according to a 4th order Runge-Kutta integration of reaction equations.

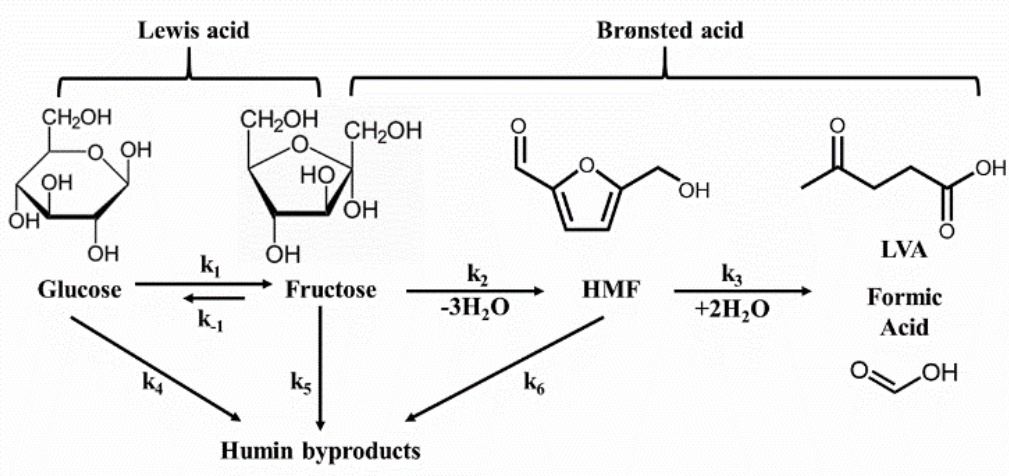

Figure 3.1. HMF Reaction Scheme Reaction pathway for the conversion of glucose to HMF. Glucose is first isomerized to fructose in a reaction catalyzed by a Lewis acid ($AlCl_3$). Then, fructose is dehydrated to HMF by maleic acid, which acts as a Brønsted acid. HMF can be additionally rehydrated to LVA. Each reactant can undergo parallel side reactions to undesired side products, known as humins. Adapted with permission from Zhang et al. 2015.[17]

3.3 Results and Discussion

3.3.1 Cosolvent screening

It has been well-established that the use of polar, aprotic solvents in combination with water increase the yield of HMF.[35–37] However, the effect of these solvents on maleic acid:$AlCl_3$ catalyst systems has not been determined. First, we performed a screen of common polar, aprotic solvents at concentrations of 10 and 20% (v/v) to determine the effect of each solvent on HMF yield from 30% (wt.) glucose **(Figure 3.2)**. The first criteria for cosolvent selection was HMF yield. DMSO resulted in the highest HMF yield from glucose, leading us to select is for further kinetic evaluation. Additionally, previous work has shown the reactions of glucose and fructose to humins to be second order.[38,39] In hopes of reducing the loss of sugars to humins throughout the reaction, we selected acetonitrile as our second solvent to evaluate due to both the reduction in unreacted glucose and reduced LVA yield. From the results of our solvent screen we hypothesized that acetonitrile altered the rate of isomerization of glucose to fructose. By combining acetonitrile with DMSO, which is known to increase the rate of fructose dehydration and inhibit HMF rehydration, we predicted that an acetonitrile:DMSO:water cosolvent system would increase sugar conversion, reduce humin formation from sugars, and increase overall HMF yield from glucose.

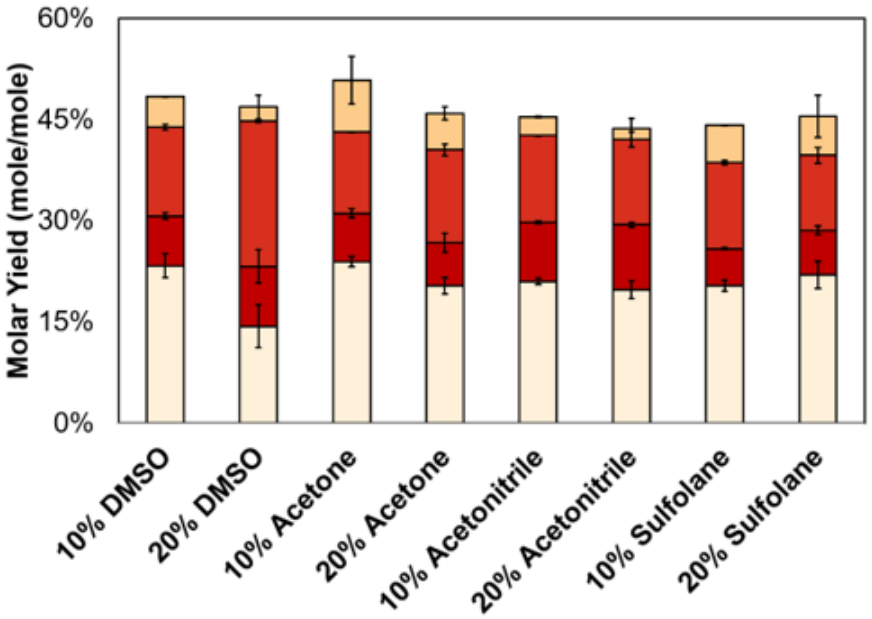

Figure 3.2. Solvent Screening Glucose remaining (white), fructose yield (red), HMF yield (orange), and LVA yield (yellow) when different solvents were used in combination with maleic acid-$AlCl_3$ catalyst system. Error bars represent the standard error of two replicates. Reaction conditions: 160 °C, 6 minutes, 30 wt. % glucose, and 100 mM $AlCl_3$.

3.3.2 DMSO increases the rate of fructose dehydration

To better understand the role of DMSO in increasing HMF yield in maleic acid and $AlCl_3$-catalyzed HMF production, we performed a full kinetic analysis of each reaction step with no DMSO, 10% DMSO, and 20% DMSO **(Figure 3.3A)**. Consistent with other works, increasing DMSO concentration led to an increase in the rate of fructose dehydration while simultaneously reducing the rate of humin and LVA formation from HMF.[21] While the altered reaction kinetics did not significantly alter the rate of glucose isomerization to fructose **(Table 3.2)**, the increased rate of fructose conversion resulted in a shift of the equilibrium concentrations of glucose and fructose towards fructose. The net effect of this was a decrease in unreacted glucose from 30% to 20% at 12 minutes for reactions with no DMSO and 20% DMSO, respectively. This increased disappearance of glucose also correlates to an increase in HMF yield from 29% to 40% when 20% (v/v) DMSO is added. The selectivity of HMF formation to HMF degradation increased from 3.3 to 13.9 with addition of 20% DMSO at 160°C.

Table 3.2. Reaction rates in DMSO Rate if each reaction step in 0, 10, and 20% DMSO at 120, 140, and 160 °C.

	Rate (min^{-1})								
	0% DMSO			**10% DMSO**			**20% DMSO**		
Rate (min^{-1})	**120°C**	**140°C**	**160°C**	**120°C**	**140°C**	**160°C**	**120°C**	**140°C**	**160°C**
k1	0.002	0.004	0.094	0.002	0.015	0.126	0.002	0.013	0.110
k2	0.004	0.031	0.250	0.010	0.037	0.356	0.003	0.041	0.555
k3	0.003	0.010	0.046	0.003	0.007	0.039	0.002	0.004	0.030
kdis	0.002	0.029	0.100	0.002	0.040	0.132	0.003	0.044	0.220
k5	0.002	0.024	0.160	0.009	0.030	0.184	0.003	0.033	0.235
k6	0.000	0.001	0.029	0.004	0.005	0.007	0.005	0.008	0.010
krev	0.001	0.000	0.020	0.000	0.000	0.012	0.000	0.000	0.025

Table 3.3. Activation Energies in DMSO Activation energies of each reaction step in 0, 10, and 20% DMSO.

		Activation Energy (kJ/mol)		
Reaction	**Symbol**	**0% DMSO**	**10% DMSO**	**20% DMSO**
Gluc to Fruc	k_1	140.9	145.2	137.9
Fruc to HMF	k_2	144.1	124.1	151.9
HMF to LVA	k_3	99.5	89.5	89.7
Glucose to Humins	k_4	1.2	1.7	1.2
Fructose to Humins	k_5	150.0	108.2	159.1
HMF to Humins	k_6	157.9	19.7	21.4
Fructose to Glucose	k_{-1}	111.5	222.3	181.6

To validate the accuracy of our kinetic model we predicted the concentration of glucose, fructose, HMF, and LVA at times outside of the initial reaction times used to determine kinetic rates **(Figures 3.3A and 3.3C)**. Activation energies for each reaction rate are shown in **Table 3.3**. For reactions conducted both with and without DMSO, the model predicts the profile of each reaction component with reasonable accuracy, confirming that our kinetic model and assumptions still accurately describe the physical system. To further validate the model, we evaluated our model against reactions performed with 30 wt. % glucose as substrate **(Figure 3.4)**. The fit of our model at elevated substrate concentrations further confirms that our assumption that each reaction is first order results in a model that can accurately predict yields, even though it has been determined experimentally that the formation of humins is second order.

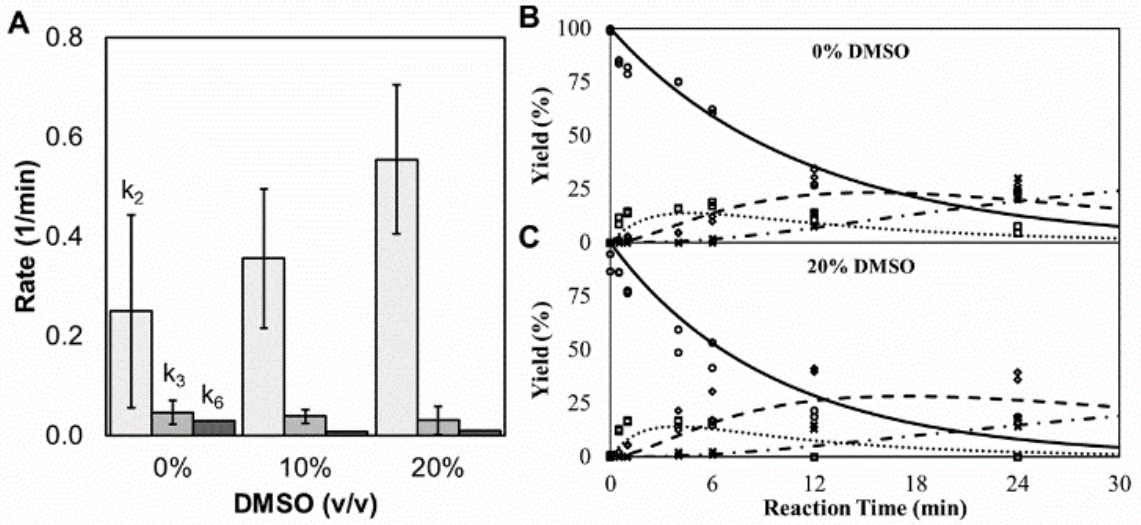

Figure 3.3. DMSO effect on kinetic rates Increasing DMSO concentration (A) alters the rate of fructose dehydration (k_2), while decreasing the rates of HMF degradation to LVA (k_3) and humin formation (k_6). Error bars represent 95% confidence intervals for kinetic rate estimate. Time-course of glucose conversion to HMF in pure water (B) and 20% (v/v) DMSO in water (C). Open shapes are observed values for glucose (circles), fructose (squares), HMF (diamonds), and LVA (crosses). Lines represent model predictions for glucose (solid), fructose (dotted), HMF (dashed), and LVA (dash and dots).

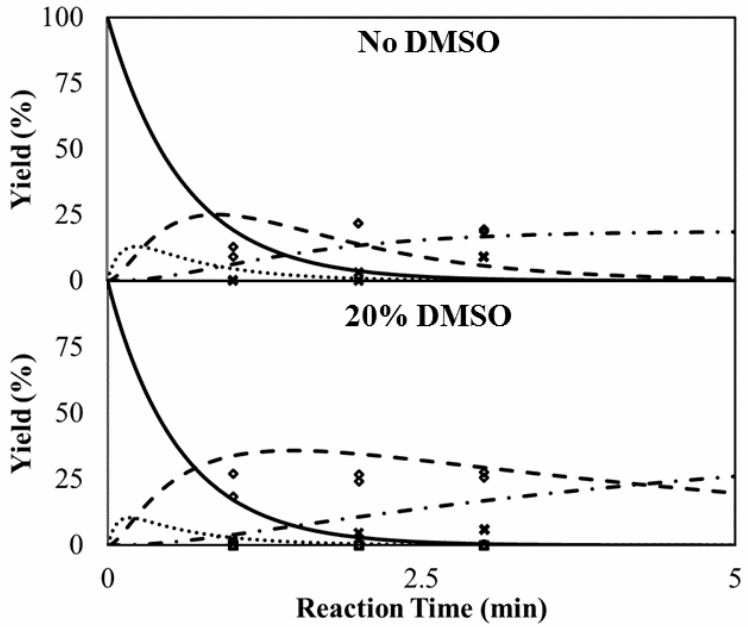

Figure 3.4. High initial glucose with DMSO Reaction of 30 wt. % glucose to HMF without DMSO (top) and with 20% DMSO in water (bottom). Lines represent simulated data for the concentration of glucose (solid), fructose (dotted), HMF (dashed), and LVA (Dashed and dotted) throughout the reaction. Points represent observed data for glucose (circles), fructose (squares), HMF (diamonds), and LVA (crosses).

3.3.3 Optimizing catalyst concentration for glucose conversion

Recent works have shown that the ratio of Brønsted acid to Lewis acid can significantly alter reaction rate, selectivity, and yield during HMF production.[40,41] In light of this information, we conducted a results-driven optimization of our catalyst system for HMF yield and glucose conversion. We first held the concentration of $AlCl_3$ constant at 100 mM and varied maleic acid concentration from 20 to 500 mM to represent ratios of 1:5, 1:2, 1:1, 2:1, and 5:1 maleic acid:$AlCl_3$ **(Figure 3.5A)**. Each of these ratios was evaluated for glucose conversion, HMF yield, and LVA yield at 160°C for 12 minutes. By evaluating the disappearance of glucose as well as the ratio of HMF yield to LVA yield, we could determine the relative rate of each catalyst ratio relative to other ratios. As maleic acid concentration was increased, the conversion of glucose was decreased significantly. This aligns with previous results which demonstrate that maleic acid likely shields glucose from further degradation.[42–44]

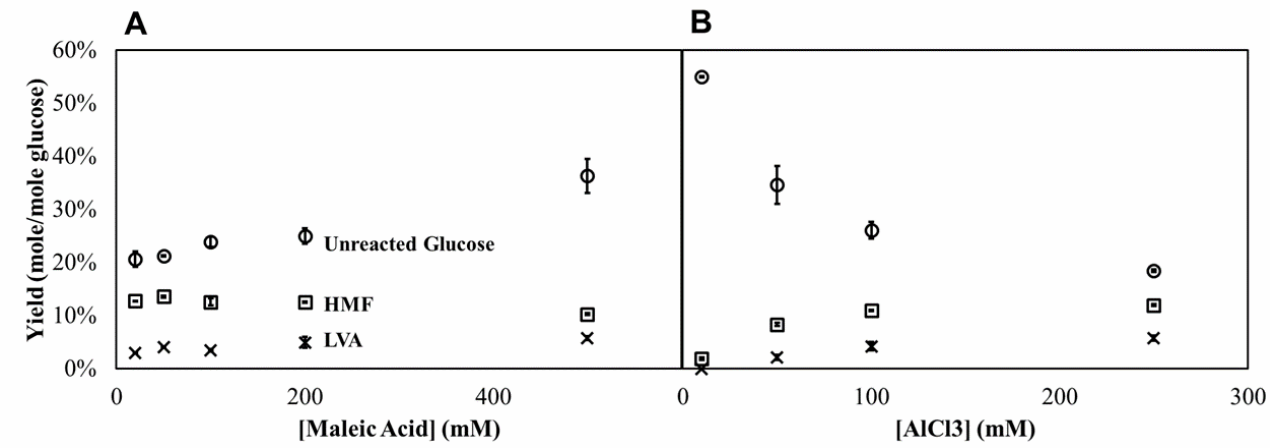

Figure 3.5. Catalyst Loading Optimization Yield of unreacted glucose (circles), HMF (squares), and LVA (crosses) with 100 mM $AlCl_3$ and varied maleic acid concentrations (A). In B, 100 mM maleic acid is used for all data, while $AlCl_3$ is varied from 20 mM to 250 mM. Error bars represent standard error of two replicate samples.

Next, the concentration of maleic acid was held constant at 100 mM while $AlCl_3$ was varied from 20 mM to 250 mM **(Figure 3.5B)**. As expected, an increase in Lewis acid concentration resulted in increased rate of glucose isomerization to fructose. However, the yield of HMF did not increase at the same rate as glucose isomerization, likely due to increased humin formation catalyzed by a high Lewis acid concentration.[41] We then conducted similar screens holding maleic acid concentration constant at 20 and 50 mM **(Figure 3.6)** to optimize the lowest catalyst loading for greatest HMF yield. From this, it was determined that greatest conversion of glucose and

highest yield of HMF was reached with an $AlCl_3$ concentration of 100 mM and a maleic acid concentration of 50 mM.

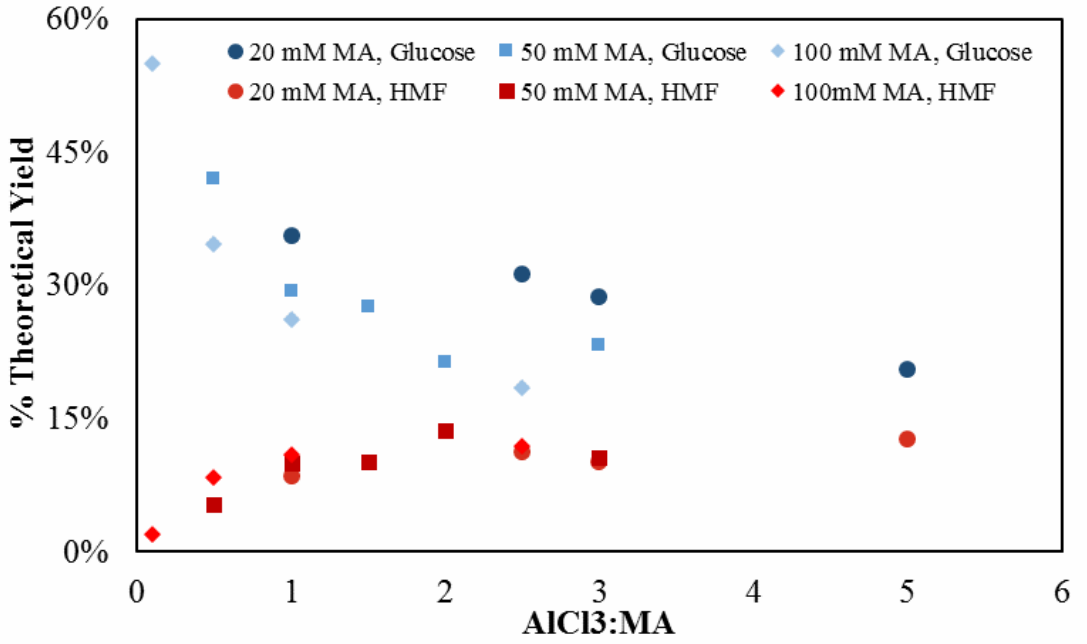

Figure 3.6. Catalyst loading optimization, continued HMF yields (red) and unreacted glucose (blue) for different ratios of $AlCl_3$ to maleic acid conducted at 160°C for 12 minutes. Maleic acid concentrations of 20 mM (Circles), 50 mM (squares), and 100 mM (diamonds) were evaluated at multiple ratios.

3.3.4 Acetonitrile increases the rate of glucose isomerization

After catalyst optimization, the use of DMSO to increase HMF yield at predicted reaction optima (195 °C, 2 minutes) was still less than 30%. This low yield was in part caused by a slow rate of glucose isomerization relative to other reactions. During our solvent screen, we had hypothesized that acetonitrile increased the rate of glucose isomerization to fructose. To test this, we performed a full kinetic evaluation of HMF production from glucose in the presence of 20 and 40% (v/v) acetonitrile in water **(Figure 3.7A)**. Interestingly, the rate of glucose isomerization is not increased substantially between 0 and 20% acetonitrile. However, at 40% acetonitrile, the rate of glucose isomerization is increased by almost 60%. Additionally, the rate of fructose isomerization to glucose was reduced by almost 50%. This suggests that acetonitrile shifts the equilibrium of glucose and fructose towards fructose. This effect on equilibrium has been described for DMSO, which stabilized the cyclic form of fructose at more than double the concentration of pure water.[21,45] However, to the best of our knowledge, this phenomena has not

been reported for acetonitrile. The increase in glucose isomerization was also accompanied by an increase in the rate of humin formation from glucose by more than 4x.

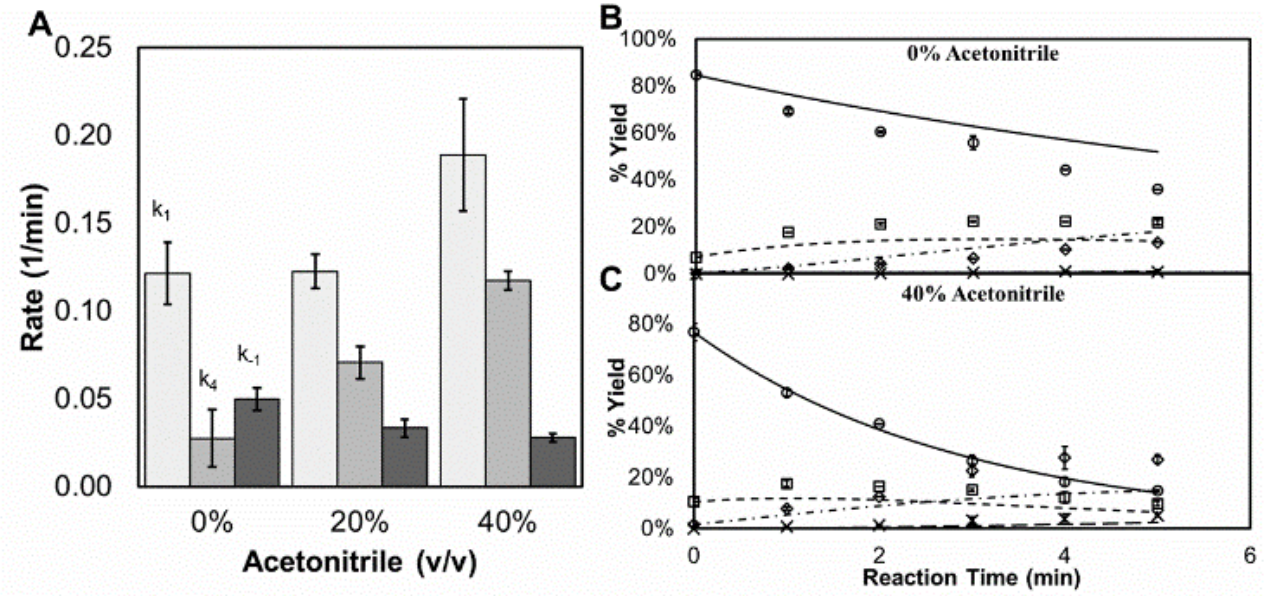

Figure 3.7. Acetonitrile Effect on Kinetic Rates Increasing acetonitrile concentration (A) increases the rate of glucose isomerization (k1). At the same time, the rate of humin formation (k_4) from glucose increases while the rate of reverse isomerization decreases (k_{-1}). Error bars represent 95% confidence interval of rate regression. HMF production as a function of time is shown for pure water (B) and 40% (v/v) acetonitrile in water (C). Open shapes are observed values for glucose (circles), fructose (squares), HMF (diamonds), and LVA (crosses). Lines represent model predictions for glucose (solid), fructose (dotted), HMF (dashed), and LVA (dash and dots). Error bars represent standard error of replicate samples.

Table 3.4. Kinetic Rates in Acetonitrile Measured kinetic rates for HMF production in 0, 20, and 40% (v/v) acetonitrile mixtures

	0% ACN			**20% ACN**			**40% ACN**		
Rate (min^{-1})	**120°C**	**140°C**	**160°C**	**120°C**	**140°C**	**160°C**	**120°C**	**140°C**	**160°C**
k_1	0.002	0.027	0.121	0.005	0.024	0.123	0.003	0.035	0.189
k_2	0.001	0.082	0.318	0.002	0.062	0.129	0.007	0.190	0.362
k_3	0.002	0.008	0.025	0.001	0.007	0.038	0.002	0.007	0.048
k_{dis}	0.005	0.033	0.108	0.005	0.039	0.259	0.012	0.087	0.350
k_5	0.007	0.044	0.142	0.006	0.028	0.043	0.017	0.073	0.074
k_6	0.001	0.014	0.050	0.001	0.001	0.055	0.001	0.002	0.050
k_{-1}	0.002	0.018	0.050	0.003	0.008	0.033	0.002	0.016	0.032

Table 3.5. Activation Energies in Acetonitrile Calculated activation energies for reaction mixtures in acetonitrile at 20 and 40% (v/v).

	Activation Energy (kJ/mol)		
	0% ACN	**20% ACN**	**40% ACN**
k1	151.3	111.9	144.1
k2	204.7	150.7	142.0
k3	98.3	115.0	118.9
k4	0.86	2.45	3.94
k5	97.8	71.6	53.6
k6	149.3	153.2	128.3
krev	118.5	91.1	88.9

While acetonitrile drastically increased the isomerization of fructose from glucose **(Table 3.4)**, it also sharply increased the production of humins from glucose. Using the calculated activation energies **(Table 3.5)**, it is seen that the activation energy for glucose isomerization with 40% acetonitrile is 144 kJ/mol, while the activation energy for glucose to humins is 4 kJ/mol. Due to this significant difference in activation energies, the expected yield of fructose from glucose increases strongly with temperature. **Figures 3.7B and 3.7C** show the fit of our predictive model to experimental data. The predictive model is generated using the Arrhenius equations to calculate the reaction rates at 160 °C, given reaction rates at 120 °C and the determined activation energies. Our model accurately predicted experimental yields, allowing us to perform optimization of reaction temperature and time for HMF production. Using the predicted optimal conditions, we evaluated the conversion of 30 wt. % glucose to HMF at 180 °C for reaction times of one and two minutes **(Figure 3.8A)**. A maximum HMF yield of 19% was reached, falling far short of the predicted 47% HMF yield from glucose. However, the model accurately predicted glucose and fructose concentrations, while failing to accurately predict the concentration of HMF and LVA. This is likely due to the formation and precipitation of HMF polymers, reducing observed HMF yield and reducing LVA yield due to substrate conversion. To test this hypothesis, we evaluated the conversion of 250 mM glucose to HMF at the same conditions **(Figure 3.8B)**. At one minute of reaction, the concentration of all products was accurately predicted, with an HMF yield of 32%. However, at two minutes, the prediction of HMF and LVA was no longer accurate, and the HMF yield was 33%, compared to a predicted 47%. From this, we concluded that HMF above a certain concentration resulted in loss of HMF to polymerization and precipitation.[38,46] This indicates that the polymerization and precipitation may be second order with respect to concentration. Above

certain concentrations, the rate of precipitation is greater than the rate of generation, acting asymptotically to HMF yield. The use of biphasic reactors may mitigate this as has been well-demonstrated for HMF previously but was beyond the scope of the present work.[7,19,21,37]

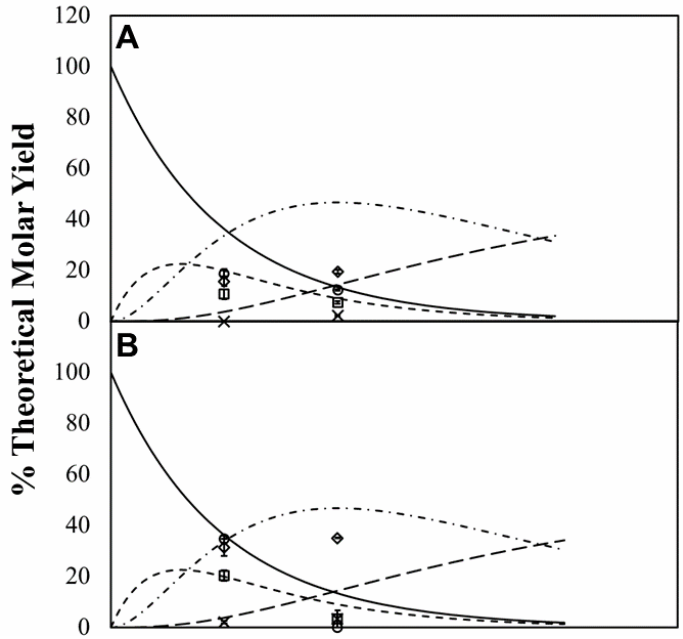

Figure 3.8. High Initial Glucose with Acetonitrile Reaction of 30 wt. % glucose to HMF in 40% acetonitrile (top) and with 250 mM glucose in 40% acetonitrile (bottom). Lines represent simulated data for the concentration of glucose (solid), fructose (dotted), HMF (dashed), and LVA (Dashed and dotted) throughout the reaction. Points represent observed data for glucose (circles), fructose (squares), HMF (diamonds), and LVA (crosses). The much better fit of HMF yields for low glucose concentrations suggests that HMF solubility is a limiting factor for HMF yield in our system.

3.3.5 Molecular dynamic simulations of glucose in water:acetonitrile mixtures

During kinetic analysis of the isomerization of glucose to fructose in acetonitrile, we observed that acetonitrile concentrations of 20% (v/v) did not significantly alter isomerization rates, while at 40% acetonitrile these rates were almost doubled. To better understand the cause of this observation we used molecular dynamic simulations to investigate differences in glucose solvation as a function of acetonitrile concentration. Since isomerization affects the position of the ring oxygen, emphasis in the analysis was focused on the ring oxygen and adjacent carbon atoms, although analysis of all carbon atoms is presented in **Figure 3.9**. Similar to prior works by Mushrif et al., the solvation of water and acetonitrile was represented by the simulated average occupancy of the oxygen in water and the nitrogen in acetonitrile around each atom of beta-glucose in the ring

form.[47–49] Using this simulation data, the radial distribution function (RDF) was evaluated for water oxygen and acetonitrile nitrogen around each carbon and oxygen atoms in glucose. By comparing the RDF of water and acetonitrile around each carbon, we could determine the relative impact of acetonitrile content on glucose solvation.

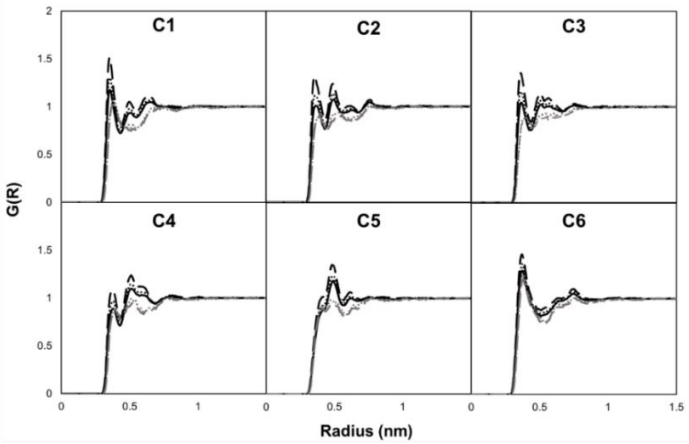

Figure 3.9. MD Simulations of Acetonitrile and Glucose RDF of water oxygen (dark lines) and acetonitrile nitrogen (gray) lines about glucose carbons 4 and 5, as well as the ring oxygen in glucose. Simulations were conducted in pure water (solid line), 20% acetonitrile (dotted lines), and 40% acetonitrile (dashed lines).

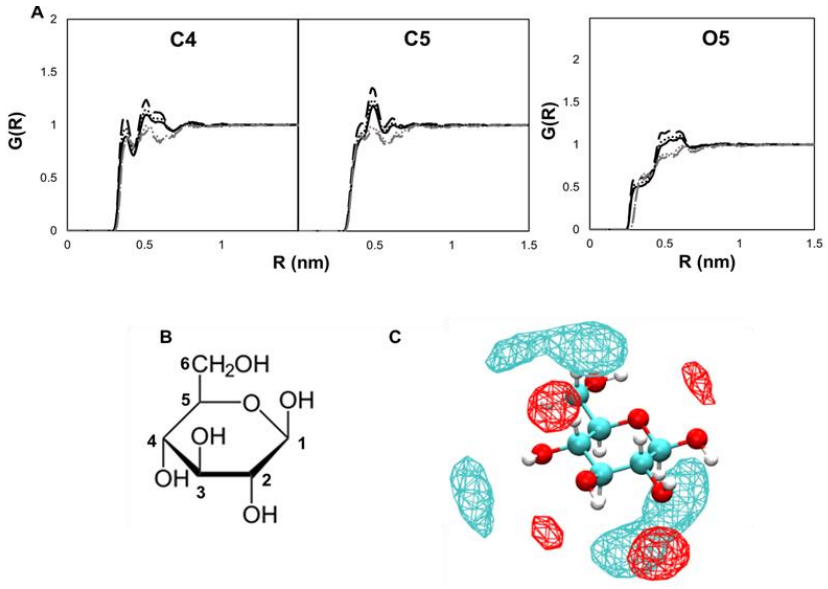

Figure 3.10. Mechanism of Acetonitrile-mediated Isomerization A) RDF of water oxygen (dark lines) and acetonitrile nitrogen (gray) lines about glucose carbons 4 and 5, as well as the ring oxygen in glucose. Simulations were conducted in pure water (solid line), 20% acetonitrile (dotted lines), and 40% acetonitrile (dashed lines). **B)** Numbering of glucose carbons used in this study. **C)** Representative visualization of the occupancy of water oxygen (blue) and acetonitrile nitrogen (red) around beta-glucose with increasing isovalues (left to right).

In all cases, it appears that two solvents compete to coordinate around the glucose indicated by the similar peak positions; however, the correlation between water and glucose appears stronger than the one between glucose and acetonitrile. **Figure 3.10A** shows the RDF for beta-glucose carbon 4, carbon 5, and oxygen 5 (ring oxygen). **Figure 3.10B** shows the numbering of carbons within the glucose ring. As acetonitrile content increases, the coordination between water and carbon 4 or 5 increases, as revealed by the stronger peak intensity of RDF. Additionally, acetonitrile competes with water in the first and second solvation shell about carbon 4. In carbon 5, there is a slight change in RDF of the glucose carbon-water oxygen pair between 0 and 20% acetonitrile. However, in 40% acetonitrile there is a significant shoulder appearing in the first peak of glucose-water at around 0.4 nm, suggesting that increasing acetonitrile content could push water 'closer' to glucose. **Figure 3.10C** shows a volumetric map of the time averaged spatial distribution of both water and acetonitrile around a glucose molecule in 40% acetonitrile solutions. The closer association of water with the ring oxygen and carbon 5 of glucose could explain the increased isomerization of glucose to fructose.[47] Additionally, the increased coordination between glucose with water in the first solvation shell with increasing acetonitrile content would explain the increased formation of humins from glucose as acetonitrile increases **(Figure 3.11)**. This is in agreement with previous work by Mushrif et al., where it was demonstrated that DMSO pushes water closer to glucose, possibly increasing the rate of side reactions to humins.[46]

3.3.6 Combining water, DMSO, and acetonitrile for HMF production

After determining that the mechanism by which acetonitrile increased HMF yield was likely different than that of DMSO, we hypothesized that combining these cosolvents into one system would reduce the amount of unreacted glucose and fructose, thus reducing humin formation and increasing HMF yield. Additionally, based on prior data suggesting DMSO may stabilize HMF in water,[48] we expected to increase the solubility of HMF through the addition of DMSO. To this end, we combined 20% (v/v) DMSO, 40% (v/v) acetonitrile, 50 mM maleic acid, and 100 mM $AlCl_3$ to produce HMF from 30 wt. % glucose **(Figure 3.11)**. As our model and MD simulations predicted, the concentrations of glucose, fructose, and LVA were reduced in the presence of both DMSO and acetonitrile. A molar HMF yield of 30% was reached at a ratio of 16.7 moles of HMF to moles of LVA. While we were able to substantially increase HMF yields relative to reactions with unoptimized catalyst in pure water, we did not drastically increase the solubility of HMF in

our reaction media. As previously described, a biphasic reaction media would greatly reduce the concentration of HMF in reaction media, increasing HMF yield. While beyond the scope of our work, future evaluation of our optimized system in a biphasic reactor configuration would likely result in substantially higher HMF yields.

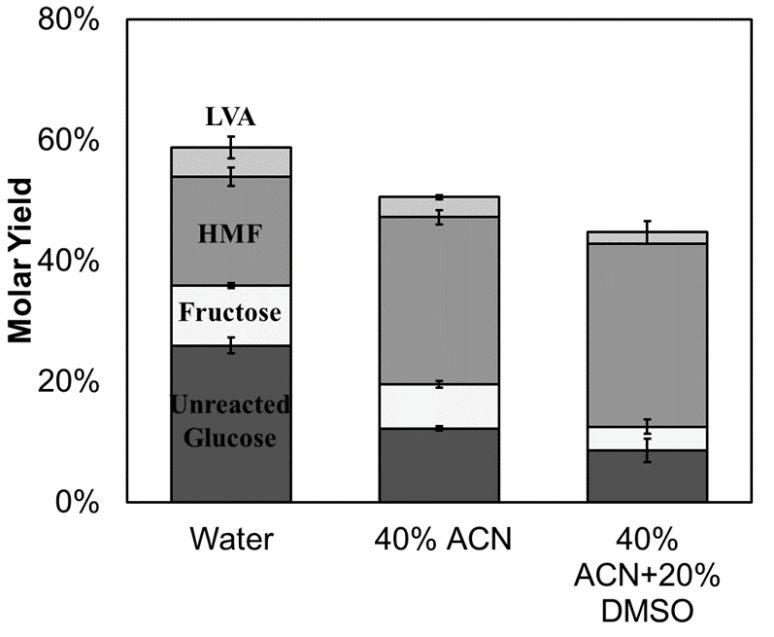

Figure 3.11. HMF Production in Acetonitrile and DMSO Molar yield of reaction components in pure water, 40% acetonitrile, and 40% acetonitrile with 20% DMSO to reduce fructose concentration throughout the reaction. Error bars represent standard error of duplicate reactions.

3.4 Conclusions

In this work we systematically evaluated solvents for increased yield and selectivity in maleic acid and $AlCl_3$-catalyzed conversion of glucose to HMF. We evaluated the impact of acetonitrile and DMSO individually on the kinetics of each reaction step. We found DMSO to more than double the rate of fructose dehydration while also strongly inhibiting rehydration of HMF to LVA. Additionally, 40% acetonitrile almost doubles the rate of glucose isomerization to fructose. To the best of our knowledge, a mechanism for how acetonitrile alters the isomerization of glucose has not been previously proposed. In light of this, we performed molecular dynamic simulations which predicted that acetonitrile increases the occupancy of water around the carbons of glucose, which we hypothesize facilitates the increased reaction rates. Using predictive kinetic models to select optimal conversion conditions, we demonstrate that HMF can be produced from

30 wt. % glucose at molar yields as high as 30%. Through additional analyses, we demonstrate that the limiting factor for HMF yield is the solubility of HMF in the reaction liquid. Through this work, we have provided a framework to reduce second order reactions of glucose and fructose to humins by reducing their concentration in the reaction mixture. This is achieved through the addition of acetonitrile to increase the rate of glucose isomerization and DMSO to increase the rate of fructose dehydration.

3.5 Acknowledgements

This material is based upon work supported as part of the Center for Direct Catalytic Conversion of Biomass to Biofuels (C3Bio), an Energy Frontier Research Center funded by the U.S. Department of Energy, Office of Science, Office of Basic Energy Sciences, and Award Number DE-SC0000997. This research was supported in part through computational resources provided by Information Technology at Purdue, West Lafayette, Indiana. The authors would additionally like to thank Casey Hooker and Pablo Vega for their helpful assistance with editing this manuscript before review.

3.6 References

1. U.S. Department of Energy. *U.S. Billion-Ton Update: Biomass Supply for a Bioenergy and Bioproducts Industry*; Oak Ridge, TN, **2011.**
2. Werpy, T.; Petersen, G. Top Value Added Chemicals from Biomass. **2004.**
3. Vijayendran, B. Bioproducts from Bio Refineries - Trends, Challenges, and Opportunities. *J. Bus. Chem.* **2010.** *9,* 109-115.
4. Wang, K.; Ou, L.; Brown, T.; Brown, R. C. Beyond Ethanol: A Techno-Economic Analysis of an Integrated Corn Biorefinery for the Production of Hydrocarbon Fuels and Chemicals. *Biofuels, Bioprod. Biorefining* **2015.** *9,* 190-200.
5. Kim, S.; Dale, B. E.; Jenkins, R. Life Cycle Assessment of Corn Grain and Corn Stover in the United States. *Int. J. Life Cycle Assess.* **2009.** *14,* 160-174.
6. Kauffman, N.; Hayes, D.; Brown, R. A Life Cycle Assessment of Advanced Biofuel Production from a Hectare of Corn. *Fuel* **2011.** *90,* 3306-3314.
7. Wettstein, S. G.; Alonso, D. M.; Chong, Y.; Dumesic, J. A. Production of Levulinic Acid and Gamma-Valerolactone (GVL) from Cellulose Using GVL as a Solvent in Biphasic Systems. *Energy Environ. Sci.* **2012.** *5,* 8199-8203.

8. Li, G.; Sun, Z.; Yan, Y.; Zhang, Y.; Tang, Y. Direct Transformation of HMF into 2,5-Diformylfuran and 2,5-Dihydroxymethylfuran without an External Oxidant or Reductant. *ChemSusChem* **2017.** *10,* 494-498.

9. Artz, J.; Mallmann, S.; Palkovits, R. Selective Aerobic Oxidation of Hmf to 2,5-Diformylfuran on Covalent Triazine Frameworks-Supported Ru Catalysts. *ChemSusChem* **2015.** *8,* 672-679.

10. Buntara, T.; Noel, S.; Phua, P. H.; Melián-Cabrera, I.; De Vries, J. G.; Heeres, H. J. From 5-Hydroxymethylfurfural (HMF) to Polymer Precursors: Catalyst Screening Studies on the Conversion of 1,2,6-Hexanetriol to 1,6-Hexanediol. In *Topics in Catalysis*; **2012.** *55,* 612-619.

11. Antonyraj, C. A.; Jeong, J.; Kim, B.; Shin, S.; Kim, S.; Lee, K. Y.; Cho, J. K. Selective Oxidation of HMF to DFF Using Ru/γ-Alumina Catalyst in Moderate Boiling Solvents toward Industrial Production. *J. Ind. Eng. Chem.* **2013.** *19,* 1056-1059.

12. Yu, I. K. M.; Tsang, D. C. W. Conversion of Biomass to Hydroxymethylfurfural: A Review of Catalytic Systems and Underlying Mechanisms. *Bioresource Technology*. **2017.** *238,* 716-732.

13. Rathod, P. V.; Jadhav, V. H. Efficient Method for Synthesis of 2,5-Furandicarboxylic Acid from 5-Hydroxymethylfurfural and Fructose Using Pd/CC Catalyst under Aqueous Conditions. *ACS Sustain. Chem. Eng.* **2018.** *6,* 5766-5771.

14. De Jong, E.; Dam, M. A.; Sipos, L.; Gruter, G. J. M. Furandicarboxylic Acid (FDCA), A Versatile Building Block for a Very Interesting Class of Polyesters. In *ACS Symposium Series*; **2012.**

15. Cubenas, G. J.; Schrader, L. F.; Ford, J. R. D. Cost of Producing High-Fructose Corn Syrup: An Economic Engineering Analysis. *United States Dept. Agric. Econ.* **1979.**

16. Marszalek, P. E.; Oberhauser, A. F.; Pang, Y. P.; Fernandez, J. M. Polysaccharide Elasticity Governed by Chair-Boat Transitions of the Glucopyranose Ring. *Nature* **1998.** *396,* 661-664.

17. Zhang, X.; Hewetson, B. B.; Mosier, N. S. Kinetics of Maleic Acid and Aluminum Chloride Catalyzed Dehydration and Degradation of Glucose. *Energy and Fuels* **2015.** *29,* 2387-2393.

18. Zhang, Z.; Wang, Q.; Xie, H.; Liu, W.; Zhao, Z. Catalytic Conversion of Carbohydrates into 5-Hydroxymethylfurfural by Germanium(IV) Chloride in Ionic Liquids. *ChemSusChem*. **2011.** *4,* 131-138.

19. Pagán-Torres, Y. J.; Wang, T.; Gallo, J. M. R.; Shanks, B. H.; Dumesic, J. A. Production of 5-Hydroxymethylfurfural from Glucose Using a Combination of Lewis and Brønsted Acid Catalysts in Water in a Biphasic Reactor with an Alkylphenol Solvent. *ACS Catal.* **2012.** *2,* 930-934.

20. Zhang, X.; Murria, P.; Jiang, Y.; Xiao, W.; Kenttämaa, H. I.; Abu-Omar, M. M.; Mosier, N. S. Maleic Acid and Aluminum Chloride Catalyzed Conversion of Glucose to 5-(Hydroxymethyl) Furfural and Levulinic Acid in Aqueous Media. *Green Chem.* **2016.** *18,* 5219-5229.

21. Chheda, J. N.; Román-Leshkov, Y.; Dumesic, J. A. Production of 5-Hydroxymethylfurfural and Furfural by Dehydration of Biomass-Derived Mono- and Poly-Saccharides. *Green Chem.* **2007.** *9,* 342-350.

22. Bicker, M.; Hirth, J.; Vogel, H. Dehydration of Fructose to 5-Hydroxymethylfurfural in Sub-and Supercritical Acetone. *Green Chem.* **2003**. *5,* 280-284.

23. Okano, T.; Qiao, K.; Bao, Q.; Tomida, D.; Hagiwara, H.; Yokoyama, C. Dehydration of Fructose to 5-Hydroxymethylfurfural (HMF) in an Aqueous Acetonitrile Biphasic System in the Presence of Acidic Ionic Liquids. *Appl. Catal. A Gen.* **2013.** *451,* 1-5.

24. Caes, B. R.; Raines, R. T. Conversion of Fructose into 5-(Hydroxymethyl)Furfural in Sulfolane. *ChemSusChem* **2011.** *4,* 353-356.

25. Abraham, M. J.; Murtola, T.; Schulz, R.; Páll, S.; Smith, J. C.; Hess, B.; Lindah, E. Gromacs: High Performance Molecular Simulations through Multi-Level Parallelism from Laptops to Supercomputers. *SoftwareX.* **2015.** *1-2,* 19-25.

26. Kony, D.; Damm, W.; Stoll, S.; Van Gunsteren, W. F. An Improved OPLS-AA Force Field for Carbohydrates. *J. Comput. Chem.* **2002.** *23,* 1416-1429.

27. Jorgensen, W. L.; Maxwell, D. S.; Tirado-Rives, J. Development and Testing of the OPLS All-Atom Force Field on Conformational Energetics and Properties of Organic Liquids. *J. of the Amer. Chem. Soc.* **1996.** *118,*11225-11236.

28. Jorgensen, W.; Chandrasekhar, J.; Madura, J.; Impey, R.; Klein, M. Comparison of Simple Water Potential Functions for Simulating Liquid Water. *J. Chem. Phys.* **1983.** *79,* 926.

29. Pothoczki, S.; Pusztai, L. Intermolecular Orientations in Liquid Acetonitrile: New Insights Based on Diffraction Measurements and All-Atom Simulations. *J. Mol. Liq.* **2017.** *225,* 160-166.

30. Hess, B.; Bekker, H.; Berendsen, H. J. C.; Fraaije, J. G. E. M. LINCS: A Linear Constraint Solver for Molecular Simulations. *J. of Comp. Chem.* **1997.** *18,* 1463-1472.

31. Essman, U.; Perera, L.; Berkowitz, M.; Darden, T.; Lee, H.; Pedersen, L. A Smooth Particle Mesh Ewald Method. *J. Chem. Phys.* **1995**. *103,* 1063.

32. Bussi, G.; Donadio, D.; Parrinello, M. Canonical Sampling through Velocity Rescaling. *J. Chem. Phys.* **2007.** *126,* 14101.

33. Parrinello, M.; Rahman, A. Polymorphic Transitions in Single Crystals: A New Molecular Dynamics Method. *J. Appl. Phys.* **1981.** *52,* 7182.

34. Humphrey, W.; Dalke, A.; Schulten, K. VMD: Visual Molecular Dynamics. **1996.**

35. Román-Leshkov, Y.; Chheda, J. N.; Dumesic, J. A. Phase Modifiers Promote Efficient Production of Hydroxymethylfurfural from Fructose. *Science.* **2006.** *312,* 1993-1997.

36. Marianou, A. A.; Michailof, C. M.; Pineda, A.; Iliopoulou, E. F.; Triantafyllidis, K. S.; Lappas, A. A. Glucose to Fructose Isomerization in Aqueous Media over Homogeneous and Heterogeneous Catalysts. *ChemCatChem* **2016.** *8,* 1100-1100.

37. Weingarten, R.; Rodriguez-Beuerman, A.; Cao, F.; Luterbacher, J. S.; Alonso, D. M.; Dumesic, J. A.; Huber, G. W. Selective Conversion of Cellulose to Hydroxymethylfurfural in Polar Aprotic Solvents. *ChemCatChem* **2014.** *6,* 2229-2234.

38. Tarabanko, V. E.; Smirnova, M. A.; Chernyak, M. Y.; Kondrasenko, A. A.; Tarabanko, N. V. The Nature and Mechanism of Selectivity Decrease of the Acid-Catalyzed Fructose Conversion with Increasing the Carbohydrate Concentration. *J. of Siberian Federal University.* **2015**. *8,* 6-18.

39. Zhang, J.; Cao, Y.; Li, H.; Ma, X. Kinetic Studies on Chromium-Catalyzed Conversion of Glucose into 5-Hydroxymethylfurfural in Alkylimidazolium Chloride Ionic Liquid. *Chem. Eng. J.* **2014.** *237,* 55-61.

40. Zhao, P.; Cui, H.; Zhang, Y.; Zhang, Y.; Wang, Y.; Zhang, Y.; Xie, Y.; Yi, W. Synergetic Effect of Brønsted/Lewis Acid Sites and Water on the Catalytic Dehydration of Glucose to 5-Hydroxymethylfurfural by Heteropolyacid-Based Ionic Hybrids. *ChemistryOpen* **2018.** *7,* 824-832.

41. Yu, I. K. M.; Tsang, D. C. W.; Su, Z.; Yip, A. C. K.; Shang, J.; Ok, Y. S.; Kim, K. H.; Poon, C. S. Contrasting Roles of Maleic Acid in Controlling Kinetics and Selectivity of Sn(IV)- and Cr(III)-Catalyzed Hydroxymethylfurfural Synthesis. *ACS Sustain. Chem. Eng.* **2018.** *6,* 14264-14274.

42. Mosier, N. S.; Ladisch, C. M.; Ladisch, M. R. Characterization of Acid Catalytic Domains for Cellulose Hydrolysis and Glucose Degradation. *Biotechnol. Bioeng.* **2002.** *79,* 610-618.

43. Lu, Y.; Mosier, N. S. Biomimetic Catalysis for Hemicellulose Hydrolysis in Corn Stover. *Biotechnology Progress*. **2007.** *23,* 116-123.

44. Ladisch, M. R.; Hendrickson, R.; Parenti, J.; Kreke, T.; Kim, Y. Fractionation of Cellulase and Fermentation Inhibitors from Steam Pretreated Mixed Hardwood. *Bioresour. Technol.* **2012.** *135,* 30-38.

45. Dais, P.; Perlin, A.S. Intramolecular hydrogen-bonding and solvation contributions to the relative stability of the beta-furanose form of D-fructose in dimethyl sulfoxide. *Carb. Res.*. **1987.** *169,* 159-169.

46. Galkin, K. I.; Krivodaeva, E. A.; Romashov, L. V.; Zalesskiy, S. S.; Kachala, V. V.; Burykina, J. V.; Ananikov, V. P. Critical Influence of 5-Hydroxymethylfurfural Aging and Decomposition on the Utility of Biomass Conversion in Organic Synthesis. *Angew. Chemie - Int. Ed.* **2016.** *55,* 8338-8342.

47. Vasudevan, V.; Mushrif, S. H. Insights into the Solvation of Glucose in Water, Dimethyl Sulfoxide (DMSO), Tetrahydrofuran (THF) and N,N-Dimethylformamide (DMF) and Its Possible Implications on the Conversion of Glucose to Platform Chemicals. *RSC Adv.* **2015.** *5,* 20756-20763.

48. Mushrif, S. H.; Varghese, J. J.; Krishnamurthy, C. B. Solvation Dynamics and Energetics of Intramolecular Hydride Transfer Reactions in Biomass Conversion. *Phys. Chem. Chem. Phys.* **2015.** *17,* 4961-4969.

49. Mushrif, S. H.; Caratzoulas, S.; Vlachos, D. G. Understanding Solvent Effects in the Selective Conversion of Fructose to 5-Hydroxymethyl-Furfural: A Molecular Dynamics Investigation. *Phys. Chem. Chem. Phys.* **2012.** *14,* 2637-2644.

4. TECHNOECONOMIC ANALYSIS AND PRELIMINARY SCALE UP OF HMF PRODUCTION FROM STARCH

The contents of Chapter 4 are adapted from the journal article "Single-vessel synthesis of 5-hydroxymethylfurfural (HMF) from milled corn", a recently published manuscript in *ACS Sustainable Chemistry and Engineering*.

4.1 Introduction

Efficient production of plastics, polyurethanes, and other polymers from renewable biomass is essential for reducing global dependence on petroleum. Globally, terephthalic acid (TPA) is the base unit for production of plastics, films, and resins – 70.3 million tonnes of TPA was consumed in 2016.[1] Traditionally, TPA is a petroleum-based, platform chemical that is produced via oxidation of paraxylene (PX). A popular use of TPA is in the production of polyethylene terephthalate (PET) – a polyester used for clothing, liquid containers, and glass fibers.[2] Recently, 5-hydroxymethylfurfural (HMF) has drawn significant interest as a bio-based platform chemical because it can undergo oxidation to produce furan-2,5-dicarboxylic acid (FDCA), a TPA substitute that can be polymerized to form bio-based plastics and polyesters.[3,4] It has been reported that some bio-based plastics have superior performance characteristics relative to petroleum-based plastics.[3]

Classically, HMF has been produced by dehydration of fructose in water or aprotic solvents, such as dimethylsulfoxide (DMSO), sulfolane, acetonitrile, and acetone.[5–10] DMSO has been found to greatly increase the selectivity of HMF production by both increasing the rate of dehydration and by blocking subsequent rehydration to levulinic acid (LVA).[5,11] Globally, fructose is produced from glucose by isomerization, and is subsequently almost three times the cost of glucose.

In part, the high cost of fructose has been a major limitation for large-scale (>20 kilotonnes per year) production of HMF.[12] In an effort to reduce cost, researchers have been working towards converting glucose to fructose and subsequently to HMF in a single-vessel reaction, reducing minimum HMF selling price from $1885 per tonne (from fructose) to $1610 per tonne (from glucose) with a capital investment of 16 M$.[13] However, this price remains prohibitive when compared with current PX selling prices of $1290 per tonne.[14] We recently demonstrated the use of the cosolvents acetonitrile (ACN) and DMSO to alter specific reaction rates in the production

of HMF.[11] Addition of 40 vol. % ACN more than doubled the rate of glucose isomerization to fructose. Additionally, 20 vol. % DMSO doubled the rate of fructose dehydration in the maleic acid:$AlCl_3$ catalyst system. Combining DMSO and ACN was expected to increase the yield of HMF from glucose; however, molar HMF yield was limited to 30% of initial glucose concentration. The low yield of HMF could be attributed to second-order polymerization reactions of HMF with sugars, humins, or reaction intermediates.[11,13] Further study was needed to determine how to overcome the unexpected low yields.

In the present work, we evaluate the impact of adding activated carbon directly to the reaction mixture on HMF yields from 30 wt. % glucose as a substrate. We apply this system to solutions containing 30% starch, liquefied corn, or milled corn. Using our experimental data, we propose an industrial production scheme and evaluate the economics of HMF production from corn to identify technical barriers that must be overcome to produce HMF at a price competitive to that of PX.

4.2 Methodology

4.2.1 Reaction conditions and catalysts

DMSO, acetonitrile, maleic acid, and $AlCl_3$ were purchased from SigmaAldrich (St. Louis, MO, USA). All reactions in this work were conducted at 180 °C with a maleic acid concentration of 0.05M and an $AlCl_3$ concentration of 0.1M. The reaction media included cosolvent concentrations of 20 vol. % DMSO and 40 vol. % acetonitrile in water. Detailed methods regarding these reactions have been described previously.[14,15] Briefly, Brønsted acids catalyze the hydrolysis of starch into the monosaccharide glucose. Glucose is then isomerized to fructose by $AlCl_3$ (Lewis acid), followed by Brønsted acid-catalyzed dehydration of fructose to HMF. HMF can be further rehydrated to levulinic acid and each reaction in has parallel side reactions to undesired side products (humins). **Figure 4.1** summarizes the reaction pathway. In all cases, substrate was loaded to at 30 wt. % and vigorously mixed before reacting. The substrates used were glucose, (Sigma Aldrich), starch (Sigma Aldrich), fermentation feed from a corn ethanol facility, and yellow dent corn milled to 1.375 mm (1/8 inch). All solid substrates were dried at 45 °C prior to use. Concentrations of reaction products were measured by high performance liquid chromatography as described in previous works.[11] A Bio-Rad Aminex H column was used with a mobile phase

consisting of 5% acetonitrile and 10 mM sulfuric acid. Components were detected by a refractive index detector (RID). Reference standards for quantification were created using pure chemical standards.

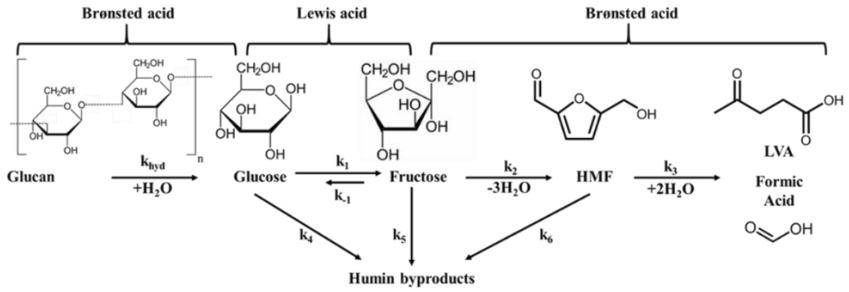

Figure 4.1. HMF Pathway from Starch Reaction schematic for conversion of starch to HMF. Brønsted acid (maleic acid) catalyzes the hydrolysis of starch. $AlCl_3$ (Lewis acid) catalyzes the isomerization of glucose to fructose. Fructose is then dehydrated to HMF, which can be rehydrated to form equimolar amounts of LVA and formic acid.

4.2.2 Techno-economic analysis

To perform an economic analysis, we designed an industrial process based on experimental data; the flow of material through the process is shown in **Figure 4.2**. In the proposed process, corn kernels are received and dried before being passed through a hammer mill, producing particles with a mean size of 3.175 mm. Ground corn is then mixed with a catalyst stream containing 0.05 M maleic acid, 0.1 M aluminum chloride, and 10 wt. % sodium chloride dissolved in 40 vol. % acetonitrile, 20 vol. % DMSO, and 40 vol. % water.

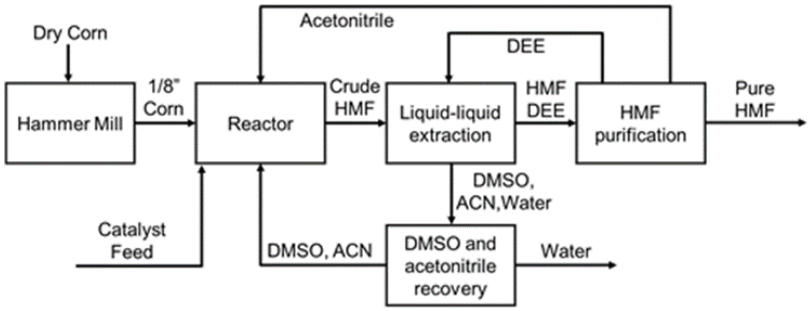

Figure 4.2. Process Flow Diagram Proposed process flow for HMF production directly from corn. Milled kernels are reacted and HMF is then removed from the reaction product by liquid-liquid extraction into an organic phase of diethyl ether (DEE). DEE is then evaporated to yield pure HMF and condensed DEE is recycled. The aqueous phase of extraction is distilled to recover acetonitrile and concentrated DMSO in water. Water removed from DMSO is a waste stream.

Salt was added to facilitate downstream separation of HMF from the reaction mixture.[16] The reactor has a retention time of three minutes and a temperature of 180°C. Multiple reactors in parallel were employed to allow for continuous operation, with some reactors dedicated to reactions while the activated carbon in remaining reactors was stripped of HMF with diethyl ether (DEE). Reaction product is sent to a liquid-liquid extractor, where DEE is used to extract HMF.[17] Experimental results indicate that 90 wt. % of HMF can be recovered in the DEE stream. DEE is then evaporated at 40 °C and 25 kPa, resulting in a pure HMF product stream. DEE is condensed and recycled. Following extraction, the stream containing acetonitrile, DMSO, salt, and water undergoes fractional distillation to recover acetonitrile while concentrating DMSO and salt. All co-solvents are recycled, and water is purged as a waste stream. All water streams containing DMSO and acetonitrile were remediated to more realistically estimate cost. A mean value of 0.11 $kWh \cdot m^{-3}$ of wastewater was assumed with a projected installed cost of 15 M$.[18] Due to uncertainty regarding the true cost of wastewater remediation, sensitivity analysis was performed regarding the cost of remediating waste water, as well as the amount of water that was discharged.

Table 4.1. TEA Conditions Plant operation and construction assumptions for economic analysis.

Plant Life	30 years
Discount Rate	10%
Depreciation	Straight Line, 10 year
Federal Tax Rate	35%
Inflation	2%
Capital Cost	43 M$
Capital Cost + Start-up Materials	180 M$
Overhead Costs (Site development, piping)	31 M$
Portion Financed	40%
Loan Conditions	10 years, 8% APR
Construction Period	1 year
Working Capital	5% of total capital investment
Start-up Period	3 months
Revenues during start-up	25%
Variable costs during start-up	100%
Fixed costs during start-up	100%
Annual Labor Cost	11 M$ per year

Site development and construction is assumed to take 9 months. Plant startup will occur over 3 months. Material costs during startup were added to the value of the initial capital loan. **Table 4.1** shows the cash flow analysis parameters used in this analysis.

The plant will be constructed during the first year of the project life with start-up commencing in year two. A 15-day supply of DMSO, acetonitrile, and DEE would be purchased up-front to accommodate start-up. At steady state, the assumed recycling efficiency of acetonitrile and DMSO is 90%, with 98% of diethyl ether being recycled. While these values were likely lower than a facility that meets federal and state waste generation regulations would operate at, overestimating high recovery values would artificially bias the minimum price point of HMF to a low value. All other capital costs were estimated using CAPCOST in Excel.[19]

Sensitivity analysis was performed using @RISK (Palisade Software, Ithaca, NY, USA) software package. **Table 4.2** shows the distributions used in sensitivity analysis. Program evaluation and review technique (PERT) distributions were used to define each variable in terms of a most likely, minimum, and maximum value. PERT distributions are a continuous distribution where the most likely value receives additional weight relative to the minimum and maximum values. Monte-Carlo analysis was performed to determine the sensitivity of financial returns to each variable. Cash flow evaluations were performed relative to the net present value (NPV) of benefits and costs over the 30-year operating life of the facility. An NPV greater than or equal to 0 is an investable project. The probability of the NPV being greater than or equal to 0 and the minimum HMF selling price to reach a mean NPV of 0 were evaluated in separate Monte-Carlo analysis with the same probability distributions.

Table 4.2. Sensitivity Analysis Conditions PERT distribution parameters used for sensitivity analysis.

Variable	Min	Mode	Max	Reference
Corn Cost [$]	3	3.75	7	Average since 2015[20]
Facility Uptime [% of 350 day year]	70%	90%	100%	Estimate
HMF Yield [g HMF/g glucose]	65%	82%	95%	Experimental Data
HMF Selling Price [$/tonne]	900	1100	1200	Competitive with PX cost[21]
HMF Recovery Efficiency	80%	90%	100%	Experimental Data
Water Recycling %	80%	90%	95%	Calculated
Acetonitrile Recycling %	90%	95%	99%	Estimate in ASPENPLUS
DMSO Recycling %	90%	95%	99%	Estimate in ASPENPLUS
DEE Recycling %	95%	98%	99%	Estimate in ASPENPLUS
Water Treatment [$/ m^3]	0.07	0.11	0.15	Estimate[18]

4.3 Results and Discussion

4.3.1 Activated carbon increases HMF yields

Recent publications indicate that acetonitrile increases the isomerization rate of glucose to fructose.[11] However, in most cases, the increased isomerization rate of glucose is matched by increased humin formation rates, likely due to a decreased average distance of water from glucose, increasing the likelihood of all reactions involving glucose and water.[11] Dumesic *et al.* demonstrated that impurities formed during dehydration of fructose interacting with glucose reduced the efficiency of isomerization.[13] To overcome the formation of impurities, Dumesic *et al.* recycled reaction media over activated carbon to maintain initial glucose conversion rates throughout multiple recycling steps.[13] To reduce the number of unit operations required within an industrial production facility, the efficacy of a single-vessel reaction of 30 wt.% glucose to HMF with 10 wt.% activated carbon added to the liquid media was tested **(Figure 4.3)**. Inclusion of activated carbon in the reaction media consisting of maleic acid, aluminum chloride, DMSO, and acetonitrile increased the molar yield of HMF from glucose almost twofold. The behavior of purified starch, enzymatically liquefied corn mash, and dry-milled corn kernels to HMF in the single-vessel reaction scheme was also evaluated.

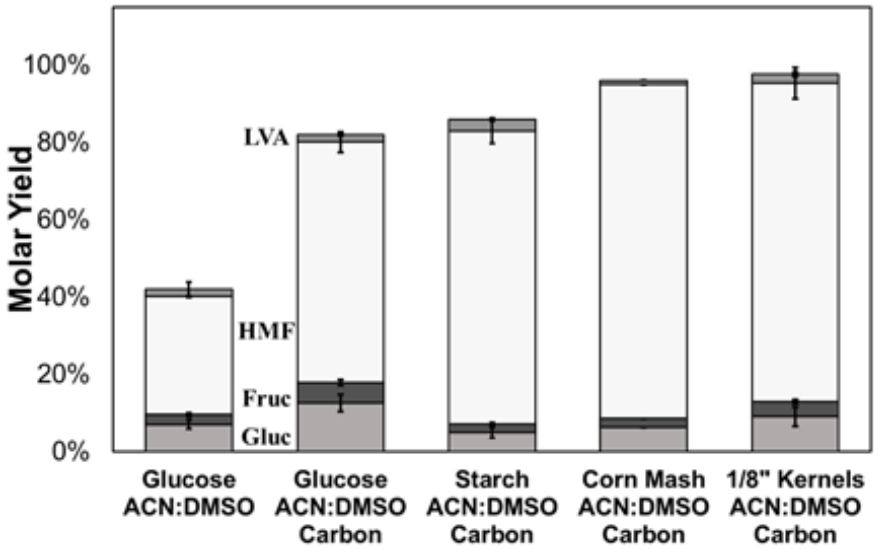

Figure 4.3. Effect of Activated Carbon on HMF Yield HMF yields in cosolvent mixtures with and without activated carbon. All substrates were loaded at 30 wt. %. Results for 30 wt. % glucose in acetonitrile and DMSO taken from Overton et al. 2019 for reference.[11] Notably, addition of activated carbon significantly increases the yield of HMF from glucose. Very high HMF molar yields are also reached from starch, corn mash, and milled corn kernels.

These reactions proceeded according to **Figure 4.1**, where starch is hydrolyzed to glucose in a reaction catalyzed by maleic acid. Glucose is then converted to HMF as described in the supplemental section. Notably, dry-milled corn kernels milled to 3.175 mm resulted in ~85% molar HMF yields. 20 to 50 mg HMF was extracted per gram of activated carbon by diethyl ether (DEE). The present findings agree with previous reports that activated carbon does not have a strong affinity for of HMF (2 - 5% by mass).[15] **Figure 4.4** demonstrates activated carbon can be recycled through four reactions with no significant loss in HMF yield. To the best of our knowledge, this is the highest HMF yield achieved from corn without the use of ionic liquids. Considering this promising data, we performed a techno-economic analysis (TEA) of an nth industrial facility to evaluate the economic feasibility of the proposed process shown in **Figure 4.2**.

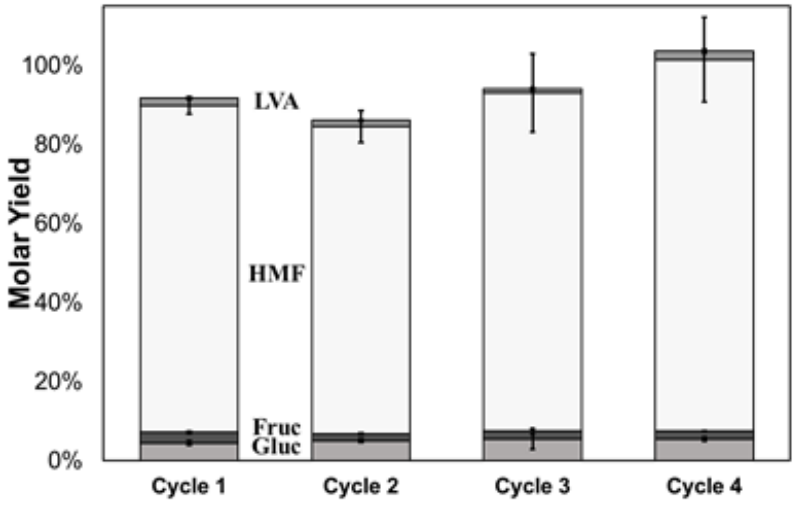

Figure 4.4. Reuse of Activated Carbon HMF yield is not reduced over 4 cycles when reusing activated carbon after a DEE wash.

4.3.2 Techno-economic analysis of a corn to HMF facility

In a static analysis, mode values from the PERT distribution (Table S2) were used. Solvent recycling efficiency was assumed to be 95%, 95%, and 98% for ACN, DEE, and DMSO, respectively. Corn cost was assumed to be $3.75 per bushel. The minimum HMF selling price was determined to be $1105 per tonne produced. This price is 85% the current cost of paraxylene.[21] The discounted payback period under these conditions was 2.5 years from plant commissioning. The sensitivity of net present value to changes in efficiency of solvent recycling, corn cost, facility uptime, HMF yield, HMF separation efficiency, and the selling price of HMF (**Figure 4.5**) was evaluated using the PERT descriptions as described in supplemental methods section of this work.

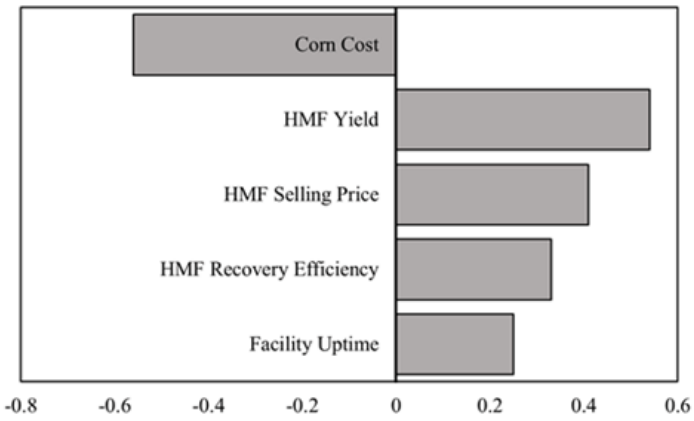

Figure 4.5. Drivers of Minimum HMF Selling Price Spearman correlation coefficients from Monte-Carlo analysis (25000 iterations) for NPV over 30 years of facility operation. Additional variables analyzed, but not shown, had correlations less than or equal to 0.01, as 99.2% of the total contribution to variance is accounted for by the five variables shown.

Corn cost, HMF yield, HMF selling price, and efficiency of HMF recovery contributed to more than 99% of the total variance in net present value (NPV) and are the most significant drivers of process profitability. Recycling of cosolvents and DEE played weaker roles in driving NPV; however, recycling efficiency is still important for meeting worker safety and environmental regulations, as well as reducing the tonnage of wastewater treated per day. The probability of having an NPV greater than or equal to 0 was 81%, suggesting that the proposed process will be very likely to generate value to shareholders, with a 50% chance of generating 254 M$ in benefits over the 30-year project term **(Figure 4.6)**.

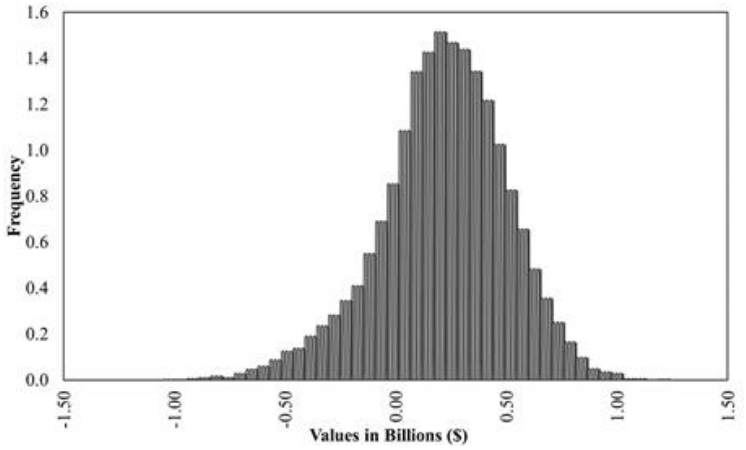

Figure 4.6. Predicted Economic Benefit Probability distribution function of NPV for Monte Carlo analysis around analyzed distributions of input variables. In this analysis, there is an 80% chance of having a positive NPV, with a median NPV of 230 M$ over the 30-year operating life of the facility.

4.4 Conclusions

In this work we have developed an efficient system for the direct conversion of milled corn kernels to the value-added product HMF. This system uses cosolvents to modify the kinetics of glucose isomerization and fructose dehydration combined with activated carbon to facilitate increased HMF yields. Corn kernels milled to 3.175 mm were converted to HMF at greater than 80% molar yields in reaction times of three minutes. In a preliminary TEA, the minimum selling price of HMF was found to be $1150 per tonne for a facility with a boilerplate capacity of 330 kilotonnes HMF per annum. Further analysis of this system outlines a clear pathway to a minimum selling price as low as $560 per tonne of HMF if very high (99%) efficiencies of solvent recycling are attained. Estimating the energy and capital costs of highly efficient systems was outside of the scope of this work, however, future work will address the design of these systems. Single-vessel conversion of corn to HMF at high yields is promising to facilitate the transition of polymer production from petroleum substrates to agricultural substrates. Based on the data presented in this work, further analysis of the technical feasibility of each unit operation should be performed at increasing scales. Here, we have established corn as a viable substrate for direct HMF production and provided a set of technical benchmarks that must be met for bio-based HMF to be sold at a price similar to petroleum-based competitors.

4.5 Acknowledgements

The authors would like to recognize funding from the Purdue Graduate School Frederick N. Andrews Fellowship, Indiana Hatch Project No. IND010677 and DOE Center for Direct Catalytic Conversion of Biomass to Biofuels (C_3Bio). Additionally, the authors recognize Jenny Stephens, Linsey Crawley, Grace Baldwin, Sabrina Overton, and Casey Hooker for assistance with sample handling, HPLC analysis of reaction products, and editing of this work. We also would like to thank Carson Reeling of Purdue Agricultural Economics for checking our cashflow analysis as part of the Agricultural Economics 608 course at Purdue.

4.6 References

1. Plastics Insights Terephthalic Acid Properties, Production, Price, and Market. https://www.plasticsinsight.com/resin-intelligence/resin-prices/purified-terephthalic-acid-pta/ (accessed March 23rd, 2019).

2. *The New Plastics Economy: Rethinking the Future of Plastics*; Technical Report for Ellen MacArthur Foundation. 2016.

3. De Jong, E., Dam, M. A., Sipos, L., Gruter, G.J. M. Furandicarboxylic Acid (FDCA), A Versatile Building Block for a Very Interesting Class of Polyesters. In *ACS Symposium Series Biobased Monomers, Polymers, and Materials*; Smith and Gross, Ed.; Washington D.C., 2012.

4. Gallo, J. M. R., Alonso, D. M., Mellmer, M. A.; Dumesic, J. A. Production and Upgrading of 5-Hydroxymethylfurfural Using Heterogeneous Catalysts and Biomass-Derived Solvents. *Green Chem.* **2013**, *15* (1), 85–90. https://doi.org/10.1039/c2gc36536g.

5. Román-Leshkov, Y., Chheda, J. N., Dumesic, J. A. Phase Modifiers Promote Efficient Production of Hydroxymethylfurfural from Fructose. *Science (80-.).* **2006**, *312*, 1933–1937.

6. Román-Leshkov, Y., Dumesic, J. A. Solvent Effects on Fructose Dehydration to 5-Hydroxymethylfurfural in Biphasic Systems Saturated with Inorganic Salts. *Top. Catal.* **2009**, *52* (3), 297–303. https://doi.org/10.1007/s11244-008-9166-0.

7. Kruger, J. S., Choudhary, V., Nikolakis, V., Vlachos, D. G. Elucidating the Roles of Zeolite H-BEA in Aqueous-Phase Fructose Dehydration and HMF Rehydration. *ACS Catal.* **2013**, *3* (6), 1279–1291. https://doi.org/10.1021/cs4002157.

8. Bicker, M.; Hirth, J., Vogel, H. Dehydration of Fructose to 5-Hydroxymethylfurfural in Sub-and Supercritical Acetone. *Green Chem.* **2003**, *5* (2), 280–284. https://doi.org/10.1039/b211468b.

9. Caes, B. R., Raines, R. T. Conversion of Fructose into 5-(Hydroxymethyl)Furfural in Sulfolane. *ChemSusChem* **2011**, *4* (3), 353–356. https://doi.org/10.1002/cssc.201000397.

10. Okano, T., Qiao, K., Bao, Q., Tomida, D., Hagiwara, H., Yokoyama, C. Dehydration of Fructose to 5-Hydroxymethylfurfural (HMF) in an Aqueous Acetonitrile Biphasic System in the Presence of Acidic Ionic Liquids. *Appl. Catal. A Gen.* **2013**, *451*, 1–5. https://doi.org/10.1016/j.apcata.2012.11.004.

11. Overton, J. C., Zhu, X.; Mosier, N. S. Molecular Dynamics Simulations and Experimental Verification to Determine Mechanism of Cosolvents on Increased 5-Hydroxymethylfurfural Yield from Glucose. *ACS Sustain. Chem. Eng.* **2019**, *7* (15), 12997–13003. https://doi.org/10.1021/acssuschemeng.9b02096.

12. Klausli, T. AVA Biochem:Commercialising renewable platform chemical 5-HMF. *Green Process Synthesis*. **2014**, 3, https://doi.org/10.1515/gps-2014-0029.

13. Motagamwala, A. H., Huang, K., Maravelias, C. T., Dumesic, J. A. Solvent System for Effective Near-Term Production of Hydroxymethylfurfural (HMF) with Potential for Long-Term Process Improvement. *Energy Environ. Sci.* **2019**, *12* (7), 2212–2222. https://doi.org/10.1039/c9ee00447e.

14. Yang, H.; Zhang, X.; Luo, H.; Liu, B.; Shiga, T. M.; Li, X.; Kim, J. I.; Rubinelli, P.; Overton, J. C.; Subramanyam, V.; et al. Overcoming Cellulose Recalcitrance in Woody Biomass for the Lignin-First Biorefinery. *Biotechnol. Biofuels* **2019**, *12* (1). https://doi.org/10.1186/s13068-019-1503-y.

15. Zhang, X.; Murria, P.; Jiang, Y.; Xiao, W.; Kenttämaa, H. I.; Abu-Omar, M. M.; Mosier, N. S. Maleic Acid and Aluminum Chloride Catalyzed Conversion of Glucose to 5-(Hydroxymethyl) Furfural and Levulinic Acid in Aqueous Media. *Green Chem.* **2016**, *18* (19), 5219–5229. https://doi.org/10.1039/c6gc01395c.

16. Altway, S.; Pujar, S. C.; de Haan, A. B. Liquid-Liquid Equilibria of Ternary and Quaternary Systems Involving 5-Hydroxymethylfurfural, Water, Organic Solvents, and Salts at 313.15 K and Atmospheric Pressure. *Fluid Phase Equilib.* **2018**, *475*, 100–110. https://doi.org/10.1016/j.fluid.2018.07.034.

17. Alam, M. I.; De, S.; Khan, T. S.; Haider, M. A.; Saha, B. Acid Functionalized Ionic Liquid Catalyzed Transformation of Non-Food Biomass into Platform Chemical and Fuel Additive. *Ind. Crops Prod.* **2018**, *123*, 629–637. https://doi.org/10.1016/j.indcrop.2018.07.036

18. Running cost of wastewater treatment plant- CostWater.com. http://costwater.com

19. Turton, R. CAPCOST. Morgantown, West Virginia 2017.

20. Corn Prices - 45 Year Historical Chart _ MacroTrends https://www.macrotrends.net/2532/corn-prices-historical-chart-data'%3ECorn Prices - 45 Year Historical Chart

21. Mellor, E. T. *Para/Ortho-Xylenes (Europe) PARA-XYLENE CONTRACT PRICES*; 2014.

22. Vinke, P., Bekkum, H. V. The Dehydration of Fructose towards 5-Hydroxymethylfurfural Using Activated Carbon as Adsorbent. *Starch* **1992**, *44*, 90–96.

5. LIQUEFACTION OF PELLETED CORN STOVER BY MALEIC ACID AND/OR ENZYMES

The contents of Chapter 5 are adapted from the journal article "New Strategy for Liquefying Corn Stover Slurries Prior to Pretreatment", a manuscript to be submitted to *Biotechnology and Bioengineering*

5.1 Introduction

Despite increasing research investment and subsidies, implementation of second generation biorefineries has been drastically limited by high investment risk. This risk is in part due to challenges with handling and feeding of solids into pretreatment reactors, as well as a lack of engineering models to design and scale equipment in lignocellulosic refineries.[1,2] While specialized reactors and compression screw feeders have been designed to feed solids into pretreatment reactors, they are still generally unreliable due to issues with plugging, compaction, and bridging of solid biomass particles.[3]

Slurries of biomass in water can be created to overcome challenges with solids feeding into pretreatment reactors. However, biomass is generally insoluble, typically limiting slurries to ~15% solids.[4] Above these concentrations, water is entrapped within the biomass and the material becomes resistant to initiation of flow (increased yield stress) and heat and mass transfer through the mixture are drastically reduced.[5,6] This creates a conundrum when combined with previous economic studies suggesting that solids contents of greater than 25% must be used to reach economically competitive ethanol selling prices.[7] While physically impractical, high solids loadings are necessary for a biorefinery to become financially practical.[8]

To overcome this challenge, previous research has evaluated strategies to reduce yield stress through partial degradation of cellulose, hemicellulose, or lignin.[5,9] However, many of these procedures have focused on the formation of a flowable slurry from pretreated biomass. This work evaluates the formation of flowable biomass slurries using enzymes, maleic acid, or a combination of both prior to pretreatment. Successful slurry creation would allow for biomass to be fed into a pretreatment reactor using conventional material handling systems, such as pumps, rather than custom feeders that substantially drive up capital costs. To the best of our knowledge, no work has focused on the creation of biomass slurries prior to the pretreatment of biomass.

In this work, we evaluate methods to decrease the yield stress of corn stover slurries at solid loadings of 30%. Importantly, a particular focus is given to processing under mild conditions to avoid significant increases in operating or capital costs. The results of this work represent an important step forward in overcoming biomass handling issues in a 2nd-generation biorefinery and are valuable for future design of lignocellulose biorefineries.

5.2 Methods

5.2.1 Corn stover harvest and processing

The corn stover used in this study, a Pioneer P0157 AMX cultivar, was harvested in Poweshiek County, Iowa, United States during the fall of 2017. Following field drying, multiple passes were made with a Hiniker windrower, cutting corn stalks at 4-in. from the soil. A Hesston 2270XD baler was used to collect the material and form 3 ft x 4 ft x 8 ft bales, which were stacked at the field-edge on a 2% slope under tarps. Bales selected from the interior of the stacks were shipped to Idaho National Laboratory (INL), where they arrived in early December.

In preparation for high-moisture densification,[10] bale moisture contents were measured using a moisture probe and the bales were adjusted to a moisture content of ca. 26% using a 2 gallon yard sprayer and allowed to equilibrate over the weekend.

The bales were then size reduced with a Vermeer BG480 hammer mill with a 7.62 cm (3-inch) screen, followed by a Bliss hammer mill fitted with a 1.11 cm (7/16-inch) screen. The milled stover was then formed into pellets using a Bliss commercial ring die pellet mill (200B-350, 5 tons hr^{-1}) with a 6 mm die diameter and an L/D ratio of eight.[10] Exposure to steam at 0.483 MPa (70 psig) for 10-30 seconds was used to preheat the milled stover at the inlet to the pellet mill to 48 °C, resulting in a pellet temperature exiting the mill of 87 °C exiting the mill. Evaporation resulted in pellets with a 15% moisture content, which were placed in super sacks for long term climate-controlled indoor storage (ambient temperature and humidity).

The chemical composition of corn stover pellets was determined according to NREL lab analytical protocols (LAPs) and is reported in **Table 5.1**.[11,12] All values except for ash content are generally consistent with previous investigations of corn stover composition.[13] Elevated ash content is likely due to increased soil particles in the corn stover caused in part by conventional three pass harvesting and reported rainy conditions during the harvest of this corn stover.

Table 5.1. Corn Stover Composition Average composition of corn stover pellets as used in this work. Standard deviation is used to show the variance in measured values.

Component	% of Total Weight
Water	6.9 ± 0.0
Glucan	23.8 ± 0.5
Xylan	12.1 ± 0.1
Arabinan	1.2 ± 0.0
Acetyl	1.3 ± 0.0
Total Lignin	11.1 ± 0.7
Ash	17.4 ± 0.0
Mass Closure	**95.7 %**

5.2.2 Enzymatic liquefaction

All reagents in this work were obtained from SigmaAldrich, unless otherwise noted. Celluclast 1.5L was purchased from SigmaAldrich and stored at in an opaque bottle at 4 °C between uses. Initial liquefactions were conducted in a 600 mL glass beaker with a wide-mouth opening. Mixing was performed by an IKA overhead stirrer out fitted with marine impellers with a blade pitch of 45 degrees were used in an up-down configuration. The bottom impeller pushed material upwards in the reactor and the top impeller pushed material downward. For 300 gram L^{-1} experiments, impellers were placed on the same axis, 5 cm apart. Beakers were submerged in a water bath to control hydrolysis temperature.

In each liquefaction experiment, 300 mL of sodium citrate buffer (100 mM, pH 4.8) were added to the beaker, followed by Celluclast 1.5L to the enzyme loading being tested and then allowed to equilibrate to liquefaction temperature for 15 minutes. After 15 minutes, the overhead mixer was started and the first batch of solids was added. Rotor speed was 300 RPM for all experiments at the 300 gram scale. Corn stover pellets were added to 30% (w/v) in a fed batch manner, with additions every 30 minutes. The first addition (t=0) was 21 grams, followed by two additions of 15 grams, one addition of 10 grams, and 7 additions of 5 grams, spaced at 30 minute intervals. The final addition was made at the end of hour 4. Following the completion of 6 hours total liquefaction time, all liquefaction materials were immediately transferred to a sealed storage container and stored at 4 °C until further analyses.

5.2.3 Maleic acid liquefaction

Maleic acid liquefaction was conducted in a 33 mL stainless steel reactor constructed from 1-inch stainless steel tubing sealed with Swagelok threaded endcap fittings as previously described.[14] Corn stover pellets were loaded to the required solids percentage (10, 15, 20, 25, or 30%) and 30 mL of maleic acid solution with the required concentration (20, 30, 40, 50, or 100 mM) was added to the reactor. Once loaded, reactors were sealed using a wrench and placed into a sand bath at a temperature of 150 °C for a total time of 36 minutes. Preliminary data had determined that these reactors took around 6 minutes to reach 150 °C, so the reaction time is considered to be 30 minutes. When the reaction time was complete, reactors were removed from the sand bath and transferred into an ice bath to cool. Treated biomass was combined and stored in a plastic screw-top bottle at 4 °C.

5.2.4 Combined liquefaction

To combine maleic acid liquefaction with enzyme liquefaction, corn stover pellets were first treated with maleic acid and then with enzyme. For this, a maleic acid concentration of 30 mM was used at a solids loading of 25% (w/v). After maleic acid treatment, solids were isolated by centrifugation at 10,000 RPM for 10 minutes, at a temperature of 4 °C and decanting off the liquid. Solids were then dried at 45 °C for 1-2 days, to a moisture content of <10% in a convection oven. It is possible that drying could hornify biomass and negatively impact enzyme hydrolysis downstream. However, this possibility is reduced by using low drying temperatures (45 °C) that should not remove bound water. Enzymatic liquefaction was conducted using these dry solids according to the same procedure described in this work. For this sample, the temperature probe was submerged to a depth of ~1 cm. The final slurry was collected in a plastic screw-top bottle and stored for rheological analysis. The reverse order of operations was also attempted, however, the citrate buffer used for enzymatic liquefaction prevented the mixture from reaching a low enough pH for substantial hydrolysis to occur.[15]

5.2.5 Yield stress measurements

Yield stress measurements of corn stover were completed using an Anton Paar MCR 702 rotational rheometer operated in a controlled shear rate mode utilizing a glass beaker measuring

cell with an inner diameter of 56mm gripped securely using the Anton Paar flexible cup holder mount. At low solids loading of corn stover (10-20% w/v), a starch cell fixture with an active length of 30mm and diameter of 24mm was used for evaluation to mitigate issues with particle settling. High solids loading samples (25-30% w/v) utilized a 4-bladed vane with a blade height of 30mm, diameter of 24mm, and blade thickness of 1mm. The gap size for both fixtures in the glass beaker setup were the same at 16mm.

Corn stover samples were placed into the measuring cell and a 15-minute rest period was allowed after lowering the fixture into the sample to mitigate effects of shear from loading. Corn stover slurries were subjected to flow curve experiments between logarithmically increasing shear rates of 0.1-100 s^{-1} to identify the relative yield stress as the maximum measured shear stress at relatively low applied shear rates.[16,17] **Figure 5.1** shows the determination of yield stress on a representative sample. Average yield stress values were plotted from 3 separate measurements and error bars indicate 1 standard deviation. In general, samples exhibited a yield stress at applied shear rates below 1 s^{-1} and then displayed shear thinning behavior as shear rate was increased beyond 1 s^{-1}.

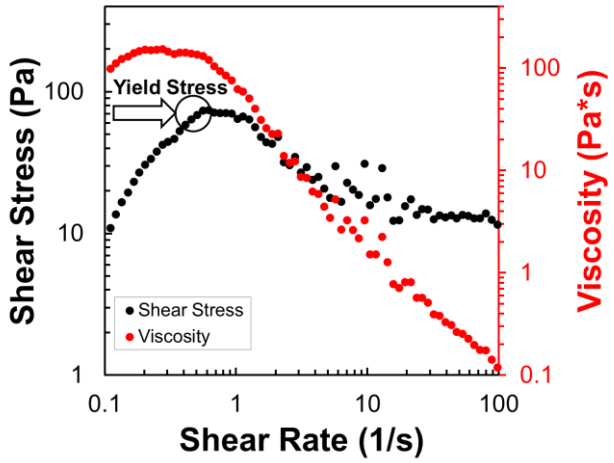

Figure 5.1. Determining Yield Stress Representative shear loading curve for corn stover slurry to demonstrate how yield stress was determined in this work.

5.3 Results and Discussion

5.3.1 Enzymatic liquefaction

Celluclast 1.5L use for liquefaction of raw biomass was evaluated at 50 °C for 6 hours at solids loadings of 10, 15, 20, 25, and 30% (w/v). **Figure 5.2** shows that Celluclast 1.5L decreases the slurry yield stress relative to controls without enzyme added. However, in both treated and untreated samples, yield stress increases exponentially with solids loading. One interpretation of this increase in yield stress is that insufficient enzyme was available to liquefy biomass at higher solids loadings (enzyme saturation). It is also possible that product inhibition limits liquefaction or that high solids loadings limit mass transfer, reducing enzyme activity and making product inhibition more likely in local regions of the reactor.[18]

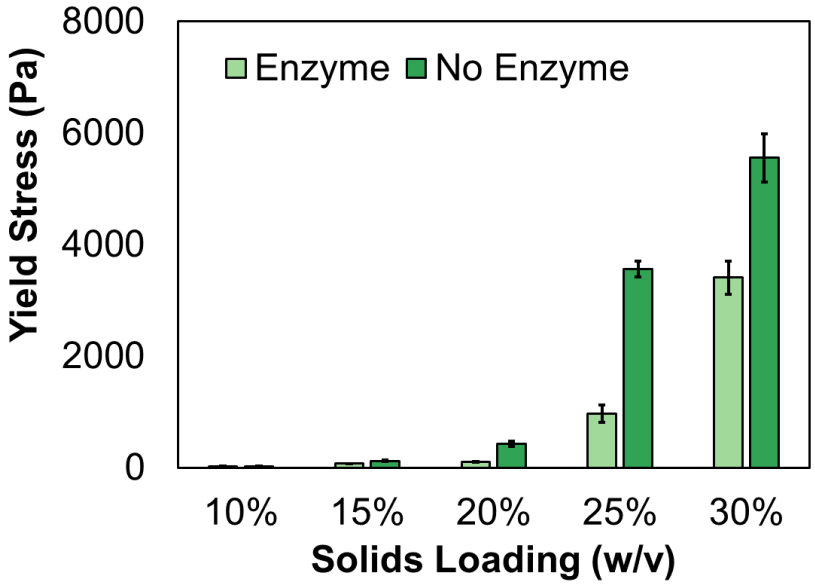

Figure 5.2. Impact of Solids on Yield Stress Addition of enzyme to corn stover pellets results in a greatly reduced (>40%) yield stress, resulting in lower energy requirements for pumping the produced slurry. Slurry yield stress increases significantly with increased solids loading. Error bars represent one standard deviation in measured yield stress.

To determine if enzyme saturation was the cause for reduced liquefaction extent, liquefaction was tested at multiple enzyme loadings for a solids content of 30% (w/v), shown in **Figure 5.3**. Additional enzyme loading did not result in reduced yield stress. In fact, yield stress reduction seems to reach an asymptote at 5 FPU per gram solids. This data suggests that enzyme inhibition (either macro- or micro-scale) and mass transfer issues were limiting liquefaction, rather than enzyme saturation. Since mass transfer and enzyme inhibition are very challenging to evaluate

independently due to their high correlation,[18] reactor scale-up was used to parse apart limiting factors of the liquefaction system. For scale-up, the assumption of constant impeller tip speed (66.8 cm s^{-1}) was used. Known impeller diameters and rotational speeds at the 300 mL scale were used to calculate impeller speed at 600 mL for a known impeller diameter. In this work, the impeller speed at 300 mL scale was 300 RPM, selected as a speed that kept particles suspended in the reactor during a visual inspection. For liquefactions at 600 mL scale, the impeller speed was 190 RPM (rounded down from the determined value of 191.7 RPM).

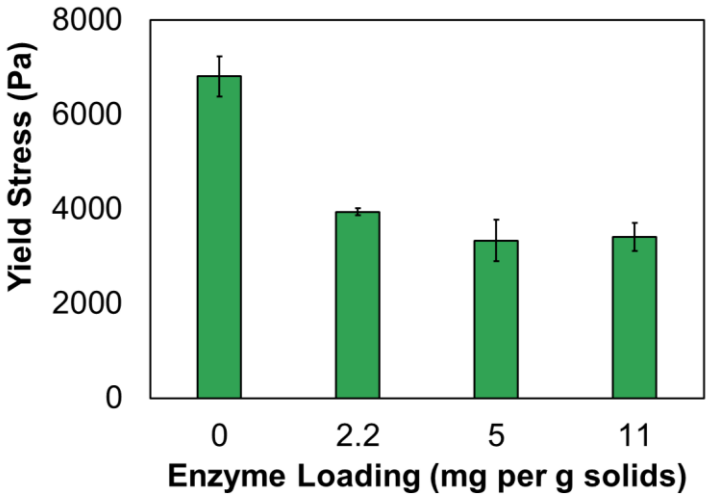

Figure 5.3. Testing Enzyme Saturation Adding additional enzyme to the liquefaction reactor does not reduce the final slurry yield stress. Error bars show standard deviation of measured slurry yield stress.

The performance of the 600 mL reactor was similar to the performance of the 300 mL reactor **(Table 5.2)**. However, visual inspection of the liquefaction reactor showed that a significant portion of the solids in the slurry were stagnating around the submerged temperature probe and trapping other particles, resulting in the formation of a stagnant 'plug' of material around the temperature probe. Due to the stagnant material in this region, the overall mass transfer in the reactor was likely reduced. To evaluate the impact of this stagnation, the temperature probe was withdrawn from the liquefaction media to a depth of <1 cm. With the probe withdrawn, resulting slurry yield stress decreased dramatically to 612 Pa. Taken together with a reduced slurry yield stress for controls with a probe depth of 1 cm, it does appear that physical disruption of corn stover particles may also play a role in reducing yield stress, albeit less substantial. These results highlight the complex interdependency of mass transfer, enzyme activity, particle physical characteristics, and free water content. While this is a 10x reduction in slurry yield stress, 612 Pa is still 20 times

greater than a 'pourable' slurry which has a yield stress around 10 Pa.[19] Given how far the enzyme system was from reaching a pourable slurry, other methods of liquefaction were evaluated.

Table 5.2. Effect of Temperature Probe on Liquefaction Measured yield stress of 30% (w/v) slurries of enzymatically liquefied corn stover and controls. Yield stress is listed as average measured value ± one standard deviation of measured yield stress.

Temperature Probe Wetted Depth (cm)	No Probe	No Probe	6 cm	6 cm	1 cm	1 cm
Scale (mL)	300	300	600	600	600	600
Enzyme Used	None	1 FPU	None	1 FPU	None	1 FPU
Yield Stress (Pa)	5556 ± 751	3334 ± 756	6054 ± 820	3659 ± 116	2232 ± 958	612 ± 112

5.3.2 Maleic acid liquefaction

Similar to Celluclast 1.5L, maleic acid can also liquefy biomass. This likely proceeds through the hydrolysis of hemicellulose in biomass.[20] Releasing this hemicellulose increases the free water content of the slurry and allows biomass particles to become 'swollen' with water.[5] Maleic acid concentrations of 20, 30, 40, 50, and 100 mM were used to liquefy corn stover at solids concentrations of 10, 15, 20, 25, and 30% (w/v) at 150 °C for 30 minutes. The yield stress for each of these samples is shown in **Figure 5.4**. Generally, increasing maleic acid concentration results in a lower yield stress, while increasing solids content increases the yield stress of the slurry. Above 25% solids, minimal free water remained in the slurry, resulting in yield stresses greater than 3000 Pa. Similar to enzyme liquefactions, even optimized conditions did not result in a 'pourable' slurry.

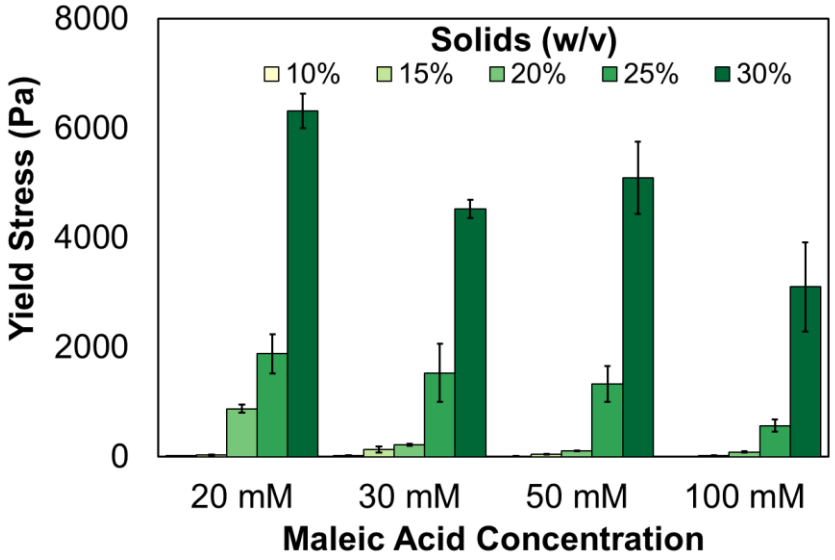

Figure 5.4. Maleic Acid Reduces Slurry Yield Stress Maleic acid treatment (150 °C, 30 minutes) reduces slurry yield stress. As with enzyme treatment, slurry yield stress increases markedly as solids content increases, but decreases as maleic acid concentration increases. Error bars represent one standard deviation of measured yield stress.

5.3.3 Combined maleic acid and enzyme liquefaction

Since the dominant mechanisms of liquefaction vary between maleic acid and enzymes, a sequential treatment process was developed to combine both liquefaction techniques. To this end, maleic acid treatment was first performed on 25% solids using 30 mM maleic acid for 30 minutes at 150 °C. After this liquefaction, the remaining solid material was centrifuged at 10,000 RPM for 10 minutes to isolate insoluble material, which was then dried to greater than 90% solids content at 45 °C. These solids were then loaded into a 1L reactor (600 mL working volume) according to the same proportionate schedule of additions as raw corn stover pellets, to a final reactor solids content of 30%. The yield stress of the final slurry (**Figure 5**) was 54 ± 21 Pa, which is relatively close to the threshold of 10 Pa for a 'pourable' slurry, and represents a greater than 100-fold reduction in yield stress relative to an untreated slurry at 30% solids (w/v).

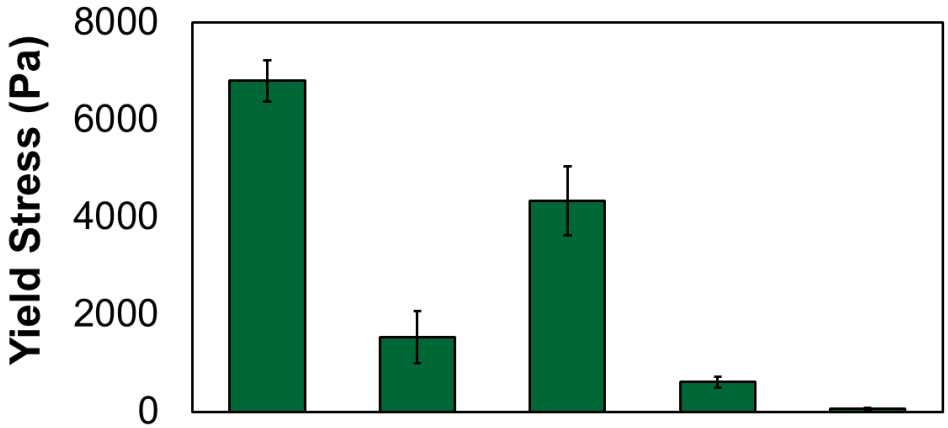

Treatment	None	Maleic Acid	Enzyme	Enzyme	Combined
% Solids (w/v)	30	30	30	30	25 → 30
1 FPU Enzyme	No	No	Yes	Yes	Second
30 mM Maleic Acid	No	Yes	No	No	First
Time (Hours)	6	0.5	6	6	0.5 → 6
Temperature (°C)	50	150	50	50	150 → 50
Scale (ml)	300	30	300	600	30 → 600

Figure 5.5. Combined Maleic Acid and Enzymatic Liquefaction Combining maleic acid treatment and enzymatic liquefaction sequentially leads to a reduced slurry yield stress relative to each treatment separately. Error bars show one standard deviation of experimentally determined yield stress values.

5.4 Conclusions

In this work, Celluclast 1.5L and maleic acid liquefaction techniques were evaluated on corn stover that had not undergone any form of pretreatment. Significantly, neither Celluclast 1.5L nor maleic acid alone is sufficient to create 'pourable' slurries of biomass at solids loadings >30% (w/v). However, in scaling Celluclast 1.5L liquefaction, the influence of local flow regimes on enzyme activity was highlighted. Specifically, the withdrawal of a temperature sensor that partially blocked flow resulted in drastically better liquefaction results in part due to better mass transfer and enzyme access to biomass. This finding highlights the significant need for models for slurry flow to be developed. Given new advances in computational power and data acquisition, it is likely that computation fluid dynamics could be used to design and optimize better reactors for liquefaction. Additional significant findings of this work are that sequential combination of maleic acid and enzyme treatment drastically decreased yield stress from >2000 Pa to 50 Pa at 30% (w/v)

solids. The resulting solids are more easily pumped and can be fed into a pretreatment reactor at higher solids content, helping to overcome some of the inherent obstacles in pretreatment. Future work concerning the development of an economic analysis should be performed in combination with optimization of the combined system for liquefaction ability and cost. In this work, we have presented a new strategy for converting raw, unpretreated biomass into a slurry for pumping in a biorefinery or for feeding into a pretreatment reactor. The findings of this work represent a significant step forward in biomass handling and address critical issues that have traditionally served as a roadblock to cost-effective pretreatment at high solids loadings.

5.5 Acknowledgements

This research was funded by the United States Department, Energy Bioenergy Technologies Office (DOE-BETO) under contract DE-EE0008256. This work was also supported by Hatch Acts 10677 and 10646, Purdue University Agricultural Research Programs, Purdue Department of Agricultural and Biological Engineering, and CAPES (DPE – Process 012981/2013-03), Brazil. Additional funding was provided to Idaho National Laboratory, operated by Battelle Energy Alliance, LLC, for the U.S. Department of Energy (DOE) under DOE Idaho Operations Office Contract DE-AC07-05ID14517. JCO would like to acknowledge funding from the Frederick N. Andrews Fellowship, provided by the Graduate School at Purdue. The authors would also like to thank Neal Yancey and Jaya Tumulurulu of Idaho National Laboratory for assisting in the bale deconstruction and palletization. The views expressed in this presentation do not necessarily represent the views of the DOE or the U.S. Government. The U.S. Government retains and the publisher, by accepting the article for publication, acknowledges that the U.S. Government retains a nonexclusive, paid-up, irrevocable, worldwide license to publish or reproduce the published form of this work, or allow others to do so, for U.S. Government purposes.

5.6 References

1. Sharma, B.; Clark, R.; Hilliard, M. R.; Webb, E. G. Simulation Modeling for Reliable Biomass Supply Chain Design Under Operational Disruptions. Front. Energy Res. 2018, 6 (September), 1–15. https://doi.org/10.3389/fenrg.2018.00100.

2. Lamers, P.; Tan, E.; Searcy, E.; Scarlata, C.; Cafferty, K.; Jacobson, J. Strategic Supply System Design - a Holistic Evaluation of Operational and Production Cost for a Biorefinery Supply Chain. Biofuels, Bioprod. Biorefining 2015, 9, 648–660. https://doi.org/10.1002/bbb.

3. Westover, T.; Hartley, D. S. Biomass Handling and Feeding. Adv. Biofuels Bioenergy 2018, 86. https://doi.org/http://dx.doi.org/10.5772/57353.

4. Hodge, D. B.; Karim, M. N.; Schell, D. J.; McMillan, J. D. Model-Based Fed-Batch for High-Solids Enzymatic Cellulose Hydrolysis. Appl. Biochem. Biotechnol. 2009, 152 (1), 88–107. https://doi.org/10.1007/s12010-008-8217-0.

5. Kristensen, J. B.; Felby, C.; Jørgensen, H. Yield-Determining Factors in High-Solids Enzymatic Hydrolysis of Lignocellulose. Biotechnol. Biofuels 2009, 2, 1–10. https://doi.org/10.1186/1754-6834-2-11.

6. Gervais, P.; Bensoussan, M.; Grajek, W. Water Activity and Water Content: Comparative Effects on the Growth of Penicillium Roqueforti on Solid Substrate. Appl. Microbiol. Biotechnol. 1988, 27 (4), 389–392. https://doi.org/10.1007/BF00251774.

7. Galbe, M.; Zacchi, G. Pretreatment of Lignocellulosic Materials for Efficient Bioethanol Production. In Biofuels; Olsson, L., Ed.; Springer Berlin Heidelberg: Berlin, Heidelberg, 2007; pp 41–65. https://doi.org/10.1007/10_2007_070.

8. Humbird, D.; Mohagheghi, A.; Dowe, N.; Schell, D. J. Economic Impact of Total Solids Loading on Enzymatic Hydrolysis of Dilute Acid Pretreated Corn Stover. Biotechnol. Prog. 2010, 26 (5), 1245–1251. https://doi.org/10.1002/btpr.441.

9. Modenbach, A. A.; Nokes, S. E. Enzymatic Hydrolysis of Biomass at High-Solids Loadings - A Review. Biomass and Bioenergy 2013, 56, 526–544. https://doi.org/10.1016/j.biombioe.2013.05.031.

10. Tumuluru, J. S. Effect of Process Variables on the Density and Durability of the Pellets Made from High Moisture Corn Stover. Biosyst. Eng. 2014, 119, 44–57. https://doi.org/10.1016/j.biosystemseng.2013.11.012.

11. Hames, B.; Ruiz, R.; Scarlata, C.; Sluiter, A.; Sluiter, J.; Templeton, D. Preparation of Samples for Compositional Analysis - Technical Report NREL/TP-510-42620. Natl. Renew. Energy Lab. 2008, No. August 1–9.

12. Sluiter, A.; Hames, B.; Ruiz, R.; Scarlata, C.; Sluiter, J.; Templeton, D.; Crocker, D. Determination of Structural Carbohydrates and Lignin in Biomass: Laboratory Analytical Procedure (LAP) (NREL/TP-510-42618). Natl. Renew. Energy Lab. 2012, No. April 2008, 17. https://doi.org/NREL/TP-510-42618.

13. Templeton, D. W.; Sluiter, A. D.; Hayward, T. K.; Hames, B. R.; Thomas, S. R. Assessing Corn Stover Composition and Sources of Variability via NIRS. Cellulose 2009, 16 (4), 621–639. https://doi.org/10.1007/s10570-009-9325-x.

14. Lu, Y.; Mosier, N. S. Biomimetic Catalysis for Hemicellulose Hydrolysis in Corn Stover. Biotechnol. Prog. 2007, 23 (1), 116–123. https://doi.org/10.1021/bp060223e.

15. Mosier, N. S.; Sarikaya, A.; Ladisch, C. M.; Ladisch, M. R. Characterization of Dicarboxylic Acids for Cellulose Hydrolysis. Biotechnol. Prog. 2001, 17 (3), 474–480. https://doi.org/10.1021/bp010028u.

16. Viamajala, S.; McMillan, J. D.; Schell, D. J.; Elander, R. T. Rheology of Corn Stover Slurries at High Solids Concentrations - Effects of Saccharification and Particle Size. Bioresour. Technol. 2009, 100 (2), 925–934. https://doi.org/10.1016/j.biortech.2008.06.070.

17. Derakhshandeh, B.; Kerekes, R. J.; Hatzikiriakos, S. G.; Bennington, C. P. J. Rheology of Pulp Fibre Suspensions: A Critical Review. Chem. Eng. Sci. 2011, 66 (15), 3460–3470. https://doi.org/10.1016/j.ces.2011.04.017.

18. Kadić, A.; Lidén, G. Does Sugar Inhibition Explain Mixing Effects in Enzymatic Hydrolysis of Lignocellulose? J. Chem. Technol. Biotechnol. 2017, 92 (4), 868–873. https://doi.org/10.1002/jctb.5071.

19. Roche, C. M.; Dibble, C. J.; Knutsen, J. S.; Stickel, J. J.; Liberatore, M. W. Particle Concentration and Yield Stress of Biomass Slurries during Enzymatic Hydrolysis at High-Solids Loadings. Biotechnol. Bioeng. 2009, 104 (2), 290–300. https://doi.org/10.1002/bit.22381.

20. Kim, Y.; Kreke, T.; Ladisch, M. R. Reaction Mechanisms and Kinetics of Xylo-Saccharide Hydrolysis by Dicarboxylic Acids. AICHE J. 2012, 59 (1), 188–199. https://doi.org/10.1002/aic.13807.

6. CONCLUSIONS AND FUTURE DIRECTIONS

6.1 Conclusions

In this work, two developments in the area of biorefining were made:

1. A method to produce HMF from starch using maleic acid and $AlCl_3$ as catalysts was developed and found to be economically viable in a preliminary economic analysis.
2. A strategy to create 'pumpable' corn stover slurries was developed using maleic acid treatment followed by enzyme hydrolysis.

Notably, HMF yields of >80% from corn were reached through the addition of activated carbon to the reactor, with an initial starch loading of 30%. This high initial loading combined with high yields led to an economically competitive minimum HMF selling price. Sensitivity analysis of the proposed process flow demonstrated that HMF yield, HMF separation efficiency, and successful operation of the plant were significant drivers of plant profitability.

Producing corn stover slurries that can easily be pumped into a pretreatment reactor are essential for reducing the high capital costs of pretreatment, as well as for reaching better mass transfer and conversion within the pretreatment reactor.

In this work, maleic acid has been demonstrated to have applications in HMF production and corn stover preprocessing. Significantly, both processes were able to use the same catalyst, a step forward in allowing biorefineries to leverage economies of scale. By lowering the per unit catalyst cost a refinery incurs, a lower operating cost can be reached. In addition, maleic acid can be used for furan production and the pretreatment of lignocellulosic material prior to enzymatic hydrolysis. The broad applicability of maleic acid to biorefining processes makes maleic acid a promising candidate for use in the biorefineries of the future.

6.2 Future Work

6.2.1 HMF production from corn kernels

While this work presented marked improvement over other works in terms of HMF yield and economic viability, the technical viability of this process has not yet been validated, particularly at scale and in regard to downstream separations. Currently, our lab is constructing a ~1 kg per day continuous reactor to produce HMF. Once this is operational, reaction parameters

will be adjusted to give the highest obtainable yields from starch. Then, downstream separations will be validated, with a particular focus on liquid-liquid extraction and the fate of co-solvents within the organic and aqueous phases. Further validation of catalyst reuse and solvent reuse will also be conducted. Using the data from these validations, a more rigorous economic model can be built in AspenPlus. This will give our lab a more detailed understanding of how this process can perform at scale, as well as help to identify critical issues that may occur during scale up.

6.2.2 Corn stover slurry formation

This work developed a new method to create corn stover slurries prior to pretreatment using maleic acid and enzymatic treatments sequentially. The resulting slurry has a yield stress of ~50 Pa, relative to an initial yield stress of 6000 Pa. Moving forward with this project, there are many interesting avenues of potential investigation. A critical area is to dive further into the behavior of solid particles in the slurry and understand how maleic acid and enzymes change these behaviors. This can be accomplished through adapting existing computational fluid dynamics (CFD) models for lignocellulose systems to incorporate changes as a function of physical characteristics. Describing the physical characteristics as a function of enzyme activity will allow this model to accurately predict changes in the flow behavior of a slurry during liquefaction. This would allow the computer-aided evaluation of different reactor geometries and conditions on final slurry properties. These insights would be directly applicable to the design and construction of 2nd generation ethanol pilot or full-scale facilities. An additional avenue of investigation is to develop an economic assessment of this liquefaction process. This could be done by integrating new data into an existing biorefinery model and performing sensitivity analysis. Determining the maximum per tonne price of preprocessing that still results in a profitable process would be essential to further evaluate and develop this liquefaction technology.

6.2.3 Combined corn refinery (CCR)

In this work, two different substrates sourced from separate parts of corn plants were used. The obvious power of this is that a corn-stover to ethanol refinery could be integrated with a corn grain to HMF refinery. An interesting work would involve the combination of both technologies into a single corn processing facility. The combined corn refinery (CCR) would further take

advantage of economies of scale by being able to use maleic acid for processing both corn and corn stover. Conceptual design and evaluation of these economics could identify future research routes, as well as create a new paradigm in how integrated biorefineries are designed.

VITA

Jonathan Christopher Overton was born in May of 1993 in Yukon, Oklahoma. He attended the Oklahoma School of Science and Mathematics, graduating in 2011. After completing high school, Jonathan worked towards his B.S. in Biosystems Engineering with an emphasis on Bioprocessing and Biotechnology at Oklahoma State University. After graduating with his B.S. degree in 2015, Jonathan remained at OSU for three months to design novel reactor systems for anaerobic fermentation. He then completed his M.S. in Biological Engineering at the University of Maine in May of 2017, investigating industrial applications of a novel self-cleaning "liquid-gated" membrane. In August of 2017, Jonathan joined the department of Agricultural and Biological Engineering at Purdue as a graduate research assistant under the Frederick N. Andrews Fellowship. During his work at Purdue, Jonathan has developed genome editing tools for anaerobic fungi, evaluated the production of platform chemicals from lignocellulosic biomass and starchy biomass, as well as evaluated liquefaction technologies to reduce pump requirements in a biorefinery. During his Ph.D. research at Purdue, Jonathan also completed a summer internship with Archer Daniels Midland Company, working as a Research Process Development Engineering Intern providing plant support and designing separation technologies for a new production process. Jonathan has received additional funding from Center for Direct Catalytic Conversion of Biomass to Biofuels (C_3Bio) and DOE Funding Opportunity Announcement (FOA) 0001689: Analytical Modeling of Biomass Transport and Feeding Systems. Jonathan began his career a Process Development Engineer with Grande Cheese Company in Fond du Lac, Wisconsin in December of 2019.

PUBLICATIONS

1. Overton, J.C., Engelberth, A.S., Mosier, N.S. 2019. Single-vessel synthesis of 5-hydroxymethylfurfural (HMF) from milled corn. *ACS Sus. Chem. And Eng.*
2. Overton, J.C., Zhu, X., Mosier, N.S. 2019. Molecular Dynamics Simulations and Experimental Verification to Determine Mechanism of Cosolvents on Increased 5-Hydroxymethylfurfural Yield from Glucose. *ACS Sus. Chem. And Eng.*
3. Yang, H., Zhang, X., Luo, H., Liu, B., Shiga, T., Li, X., Kim, J.I., Rubinelli, P., Overton, J.C., Subramanyam, V., Cooper, B.R., Mo, H., Abu-Omar, M.M., Chapple, C., Donohoe, B., Makowski, L., Mosier, N.S., McCann, M.C., Carpita, N.C., Meilan, R. 2019. Overcoming cellulose recalcitrance in woody biomass for the lignin-first biorefinery. *Biotechnology for Biofuels.*
4. Hooker, C, Hillman, E.T., Overton, J.C., Ortiz-Velez, A., Schacht, M., Hunnicut, A., Mosier, N.S., Solomon, K.V. 2018. Hydrolysis of untreated lignocellulosic feedstock is independent of S-lignin composition in newly isolated anaerobic fungus, *Piromyces spp.*. *Biotechnology for Biofuels.*
5. Overton, J.C., Weigang, A., Howell, C. 2017. Passive Flux Recovery in Protein-Fouled Liquid-Gated Membranes. *Journal of Membrane Science*.
6. Kovalenko, Y., Sotiri, I., Timonen, J. V. I., Overton, J.C., Holmes, G., Aizenberg, J., Howell, C. 2016. Bacterial Interactions with Immobilized Liquid Layers. *Advanced Healthcare Materials*.
7. Sotiri, I., Overton, J.C., Waterhouse, A., Howell, C. 2016. Immobilized liquid layers: a new approach to anti-adhesion surfaces for medical applications. *Invited mini review accepted to Experimental Biology and Medicine.*
8. Liu, K., H. K. Atiyeh, O.P. Planas, T. Ezeji, V. Ujor, Overton, J.C., K. Berning, M. R. Wilkins, and R. S. Tanner. 2015. Butanol Production from Hydrothermolysis-Pretreated Switchgrass: Quantification of Inhibitors and Detoxification of Hydrolyzate. *Bioresource Technology*.